



HASP Student Payload Application for 2022

Payload Title: Measurements of Good Ozone in the Stratosphere and Bad Ozone in Troposphere using improved sensors payload.			
Institution: University of North Florida (UNF) and University of North Dakota (UND)			
Payload Class: SMALL		Submit Date: 01/05/2022	
Project Abstract:			
<p>Good ozone in the stratosphere protects us from the Sun's harmful ultraviolet rays. However, bad ozone in the troposphere, closer to Earth's surface, is a pollutant and hazardous to our health. Based on the success and experience of previous HASP flights, the UNF-UND team proposes the HASP 2022 flight for the fabrication of new improved design of ozone sensors payload to measure good ozone profile in the stratosphere and bad ozone in the troposphere. Three different types of nanocrystalline and nanocomposite materials will be used in fabrication of thin film gas sensors arrays. Gas sensors will be mounted on the three sides of rectangular payload body. Each sensor box will have 8 ozone gas sensors array. Ozone gas sensors will be fabricated and calibrated by the students' team at UNF. The UV light photodiode sensor will be mounted just below ozone gas sensors box to measure the amount of photovoltage generated by UV sun light, which will support the science concept of generation of ozone gas in the presence of UV sun light. This proposed HASP2022 flight science experiment will help us understanding good ozone in the stratosphere, bad ozone in the troposphere and any possible observation of higher concentration of ozone due to nocturnal ozone maxima after termination of flight at nighttime.</p>			
Team Name: Ozone Sensors		Team or Project Website: N/A	
Student Team Leader Information:		Faculty Advisor Contact Information:	
Name:	Miguel Bolante (Leader)	Dr. Nirmalkumar G. Patel	Dr. Ronald Fevig
Department:	Physics	Physics	Space Studies
Mailing Address:	University of North Florida Building #50 1 UNF Drive	University of North Florida Building #50 1 UNF Drive	University of North Dakota Clifford Hall, Room 512 4149 Uni. Ave Stop 9008
City, State,	Jacksonville, FL 32224	Jacksonville, FL 32224	Grand Forks, ND 58202
Email:	N01434191@unf.edu	npatel@unf.edu	rfevig@space.edu
Office Telephone	904-620-2729	904-200-2855	701-777-2480
Mobile Telephone	904-482-3673	904-200-2855	520-820-3440

HASP2022 Proposal

**Measurements of
Bad Ozone in the Troposphere and
Good Ozone in the Stratosphere using
improved sensors**

Submitted by



University of North Florida (UNF) and University of North Dakota (UND)

UNF Students Team:

Miguel Bolante (Leader)
Karli Dattilo
Diego Fontan-Ulibarri
Michael Shearer

Faculty Advisors:

Dr. Nirmalkumar G. Patel (UNF)
Dr. Ronald A. Fevig (UND)

Table of Contents		
Section	Content	Page
	Flight Hazard Certificate Checklist	4
1	Payload Description	5
1.1	Payload Scientific / Technical Background	5
1.1.1	Mission Statement	8
1.1.2	Mission Background and Justification	9
1.1.3	Mission Objectives	12
1.2	Payload Systems and Principle of Operation	15
1.3	Major System Components	19
1.4	Mechanical and Structural Design	19
1.5	Electrical Design	22
1.6	Thermal Control Plan	23
2	Team Structure and Management	27
2.1	Team Organization and Roles	27
2.2	Timeline and Milestones	28
2.3	Anticipated Participation in Integration and Launch Operation	30
3	Payload Interface Specifications	31
3.1	Weight Budget	31
3.2	Power Budget	32
3.3	Downlink Serial Data	36
3.4	Uplink Serial Commanding	37
3.5	Analog Downlink	38
3.6	Discrete Commanding	38
3.7	Payload Location and Orientation Request	38
3.8	Special Request	39
4	Preliminary Drawings and Diagrams	40
5	References	40
	Appendix-A Detailed Mechanical Drawings	41
	Appendix-B Detailed Electronic Circuit Diagrams	56


Flight Hazard Certification Checklist

NASA has identified several classes of material as hazardous to personnel and/or flight systems. This checklist identifies these documented risks. Applying flight groups are required to acknowledge if the payload will include any of the hazards included on the list below. Simply place an (x) in the appropriate field for each hazard classification. **Note:** Certain classifications are explicitly banned from HASP (grey filled items on table below) and the remaining hazards will require additional paperwork and certifications. If you intend to include one of the hazards, you must include detailed documentation in section 3.8 of the application as required by the HASP Call for Payloads.

This certification must be signed by both the team faculty advisor and the student team lead and included in your application immediately following the cover sheet form.

Hazardous Materials List		
Classification	Included on Payload	Not Included on Payload
RF transmitters		X
High Voltage		X
Lasers (Class 1, 2, and 3R only) Fully Enclosed		X
Intentionally Dropped Components		X
Liquid Chemicals		X
Cryogenic Materials		X
Radioactive Material		X
Pressure Vessels		X
Pyrotechnics		X
Magnets less than 1 Gauss		X
UV Light		X
Biological Samples		X
Batteries		X
High intensity light source		X

Student Team Leader Signature: 
 (Miguel Bolante)

Faculty Advisor Signature: 
 (Dr. Nirmal G. Patel) 01/05/2022

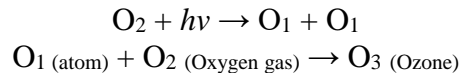
1. Payload Description

1.1 Payload Scientific /Technical Background

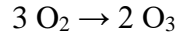
Ozone in the stratosphere protects us from the Sun's harmful ultraviolet rays. However, ozone in the troposphere, closer to Earth's surface, is a pollutant and hazardous to our health. We take 20,000 breaths a day. The air we breathe has a huge impact on our health.

Good Ozone in the Stratosphere

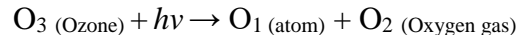
Generation of Ozone in the Stratosphere: Oxygen gas (O_2) is present in the atmosphere. High energy or shorter wavelength UV light ($h\nu$) collides with the oxygen molecule (O_2), causing it to split into two oxygen atoms. These atoms are unstable, and they prefer being "bound" to something else. The free oxygen atoms then smash into other molecules of oxygen, forming ozone (O_3).



The overall reaction between oxygen and ozone formation is:



The ozone is destroyed in the process that protects us from UV-B and UV-C rays emitted by the Sun. When ozone (O_3) absorbs UV light ($h\nu$), it will split the molecule into one free oxygen atom (O_1) and one molecule of oxygen gas (O_2). Thus, absorption of UV-B and UV-C leads to the destruction of ozone



Ozone is valuable to us because it absorbs harmful UV radiation during its destruction process. A dynamic equilibrium is established in these reactions. The ozone concentration varies due to the amount of radiation of light received from the sun.

Bad Ozone in the Troposphere

Generation of Ozone in the Troposphere: Ozone in the troposphere is bad. This ozone is contributing to the smog and greenhouse gases created by human activities. Ozone close to the ground surface does not exist in high enough concentrations to shield us from UV light.

Formation of tropospheric ozone

- involved are VOC (RH), OH (hydroxyl radical), NO_x , M (inert body, N_2 , or O_2); O_3 can be dissociated by UV and will form two OH \rightarrow chain process
- VOC and NO_x concentrations control ozone concentrations in a complicated way
- O_3 formation is probably NO_x limited, rather than VOC

The formation of tropospheric ozone required:

- VOCs: volatile organic compounds: mostly emitted by motor vehicles, vegetation, industrial, and commercial, dry cleaners, paints
- NO_x : nitrogen oxides, motor vehicles, power plants, industrial facilities, biomass burning, lightning. Sunlight, higher temperature, and low wind speed

Tropospheric ozone affects the meteorology

- higher O₃ concentrations can be found in the summer during dry high-pressure conditions
- during inversions (warm air above cooler air) pollutants often get trapped resulting in high ozone concentrations and form nocturnal ozone maxima at nighttime.

Tropospheric, or ground-level ozone, is the major ingredient in smog and continues to pose a health risk.

- ozone attacks cell and breaks down tissue
- decreased ability to breathe, coughing, increased susceptibility to respiratory diseases such as pneumonia and bronchitis
- increased sensitivity to allergens
- long-term exposure may result in permanent lung damage
- according to EPA, about 15,000 Americans die every year from exposure to air-borne pollutants, and exposure to ozone causes hundreds of thousands of acute asthmas
- ozone is a plant toxin, enforced by presence of SO₂ and NO_x
- ozone also damages materials such as nylons, rubber, and certain fabrics
- economic impacts
- damage of agricultural crops, forests, and wilderness areas
- Lowering of ozone levels by 25% may increase US crop yield by \$0.5 to 1.0 billion per year.
- Natural tropospheric ozone concentration: 10 ppb. However, higher level is bad for health.

In establishing the 8-hour standard, EPA is setting the standard at 0.08 parts per million (ppm) and defines the new standard as a "concentration-based" form, specifically the 3-year average of the annual 4th-highest daily maximum 8-hour average ozone concentrations.

Ozone Hole

The criticality of ozone layer can be understood from the fact that, only 10 or less of every million molecules of air is ozone. Most of these ozone molecules reside in a layer between 10 and 40 kilometers above the surface of the Earth known as stratosphere. Each spring in the stratosphere over Antarctica (spring in the southern hemisphere is from September through November.), atmospheric ozone is rapidly destroyed by chemical processes. As winter arrives, a vortex of winds develops around the pole and isolates the polar stratosphere. When temperatures drop below -78°C, thin clouds form of ice, nitric acid, and sulfuric acid mixtures. Chemical reactions on the surfaces of ice crystals in the clouds release active forms of CFCs. Ozone depletion begins, and the ozone "hole" appears. About 50% of the total column amount of ozone in the atmosphere disappears during two to three months. At some levels, the losses approach 90%. This has come to be called the Antarctic ozone hole. In spring, temperatures begin to rise, the ice evaporates, and the ozone layer starts to recover.

Thus, ozone “hole” is a reduction in concentrations of ozone high above the earth in the stratosphere. The ozone hole is defined geographically as the area wherein the total ozone amount is less than 220 Dobson Units. The ozone hole has steadily grown and length of existence over the past two and half decades. Now, the size of ozone hole over Antarctica is estimated to be about 30 million sq. km. It has been observed that, man-made chlorines, primarily chlorofluorocarbons (CFCs), contribute to the thinning of the ozone layer and allow larger quantities of harmful ultraviolet rays to reach the earth.

Nocturnal Ozone

The observed higher concentration of ozone at nighttime due to nocturnal ozone maxima observed in ozone episode areas as a bad ozone can be correlated with vertical mixing of remnant daytime boundary layer. This mixing is forced by an increase in wind speed above the nocturnal surface inversion (fig 1 (a)). Samson [1] proposed that this process not only explains nighttime increases in ozone concentrations at lower altitude and process responsible for the reversed diurnal ozone fluctuations at higher altitude. Numerous investigators [2-3] have shown that higher ozone concentration occur on the back side of surface high pressure systems where the air, circulating poleward, has above average dry-bulb and dew point temperatures.

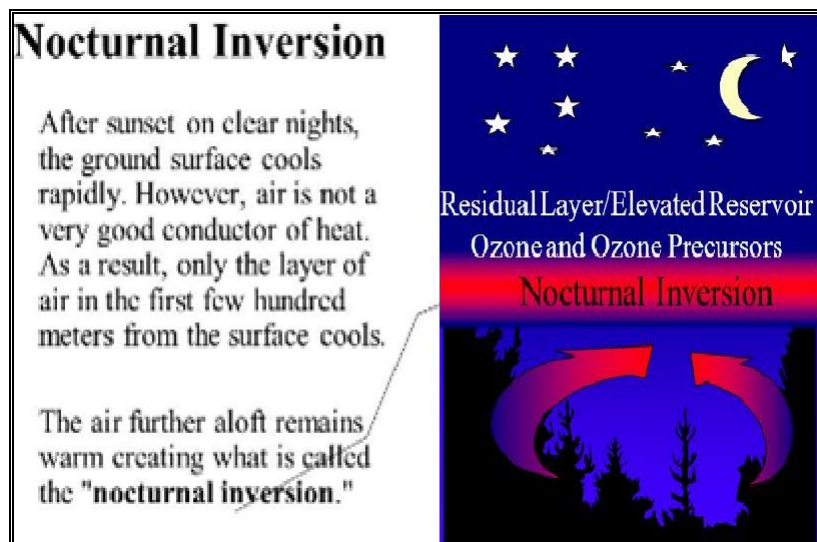


Fig. 1 (a) Formation of Nocturnal Ozone
 Courtesy: <http://slideplayer.com/slide/5314464/>

Looking into this global issue of bad ozone and ozone depletion, we are working on the development of space grade ozone sensors and low weight sensors payload to measure the ozone profile in the stratosphere on the real time mode using the NASA-HASP balloon flight since 2008. The purpose of development of reliable low cost and miniature nanocrystalline

thin film ozone sensor is to substitute the conventional tools such as bulky and expensive Dobson spectrophotometer, light detection and ranging (LIDAR), Satellite ultraviolet backscatter, Ozone sondes and electrochemical based sensors. Most of commercially available electrochemical based ozone sensors have disadvantages of (i) not good for space application due to effect of humidity and pressure on sensor, (ii) sensitive to electromagnetic and radio frequency interferences, (iii) limited sensors lifetime and (iv) less accuracy at low ozone levels (below 1 ppm). Spectrometer based ozone detection systems have disadvantages of (i) higher cost, (ii) physically larger in size, (iii) bench mount and not handheld and (iv) slow measurements.

1.1.1 Mission Statement

Nanocrystalline oxide semiconductor thin films gas sensor arrays technology (U. S. Patent No. 10,823,690 B2, and 9,606,078 B2) and ITO-QCM (Quartz Crystal Microbalance) sensor platform technology (U.S Patent No. 7,930,923 B2) were developed by Dr. Patel at the University of North Florida (UNF) for the detection of ozone, toxic gases, explosive materials, and chemical warfare agents with support of the Edgewood Chemical Biological Center, US Army Laboratory, Aberdeen Proving Ground and the U.S. Department of Defense. Nanocrystalline gas sensors have also been used for the detection of ozone gas in the stratosphere. Nanocrystalline indium tin oxide (ITO) gas sensors were successfully first time tested and calibrated with ozone gas at the Kennedy Space Center (KSC) and at the UND during 2008-2009 [4]. UNF team is improving the performance of ozone sensors by changing its fabrication conditions and modifying its surface structure every year after HASP balloon flight. These sensors were successfully tested on HASP 2008 to 2021 flights. We have made step by step improvement of sensors by changing sensing materials, design and fabrication parameters, and hardware and software of the payload every year. UNF ozone sensors were also used by the students at Louisiana State University, University of Central Florida, Iowa State University and Taylor University for their weather balloon projects.

The proposed mission is the fabrication of new improved ozone gas sensors payload. The new payload has several unique features. ITO gas sensor arrays have higher sensitivity and stability because of the nanocrystalline and nanocomposite thin film structure. Earlier reported work on tungsten oxide sensors for the detection of ozone gas [5] required a high operating temperature of about 450°C to detect ozone, while the UNF developed nanocrystalline ITO sensors arrays operate at the room temperature and do not require a heater, which ultimately saves power requirements and space, and minimizes the possibility of an accidental fire. The UNF developed alpha phase of silver tungstate thin film gas sensors have better sensitivity and selectivity for detection of ozone gas at low pressure, while nanocomposite WO_{3-x} +ITO and Al doped ZnO+ITO thin film gas sensors have better selectivity for detection of ozone in pollutant gases and smog. UNF developed gas sensors arrays are very small in size, have low weight and low power consumption, which meets the payload requirements for the space applications. These gas sensors can easily be integrated with microcontroller electronic circuits. Compared to the conventionally costly spectroscopic and other reference methods for the detection of ozone, our gas sensors payload has

low cost and low weight for the rapid and real time detection of ozone in the troposphere and stratosphere.

1.1.2 Mission Background and Justification

Pervious HASP Flight

The proposed work is in continuation of the previous last two HASP flights. Overview of output of the last HASP 2021 flight is given in fig.1 (b). The picture of ozone sensors payload, payload-HASP in stratosphere and the flight profile are also shown in fig. 1(b). The response of UV photo sensors mounted on three sensors boxes are shown in fig. 1 (c).

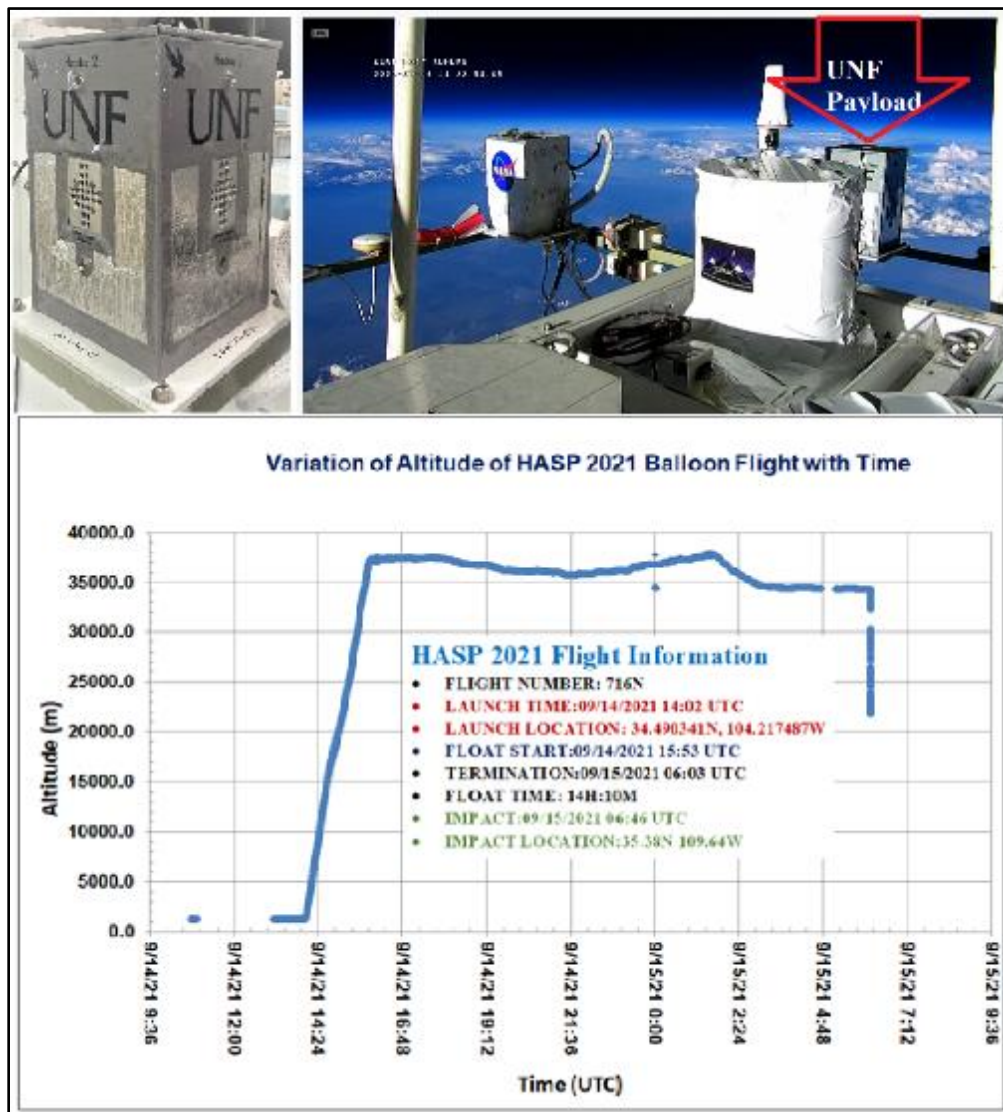


Fig. 1(b) HASP 2021 payload, HASP in Stratosphere and balloon flight profile.

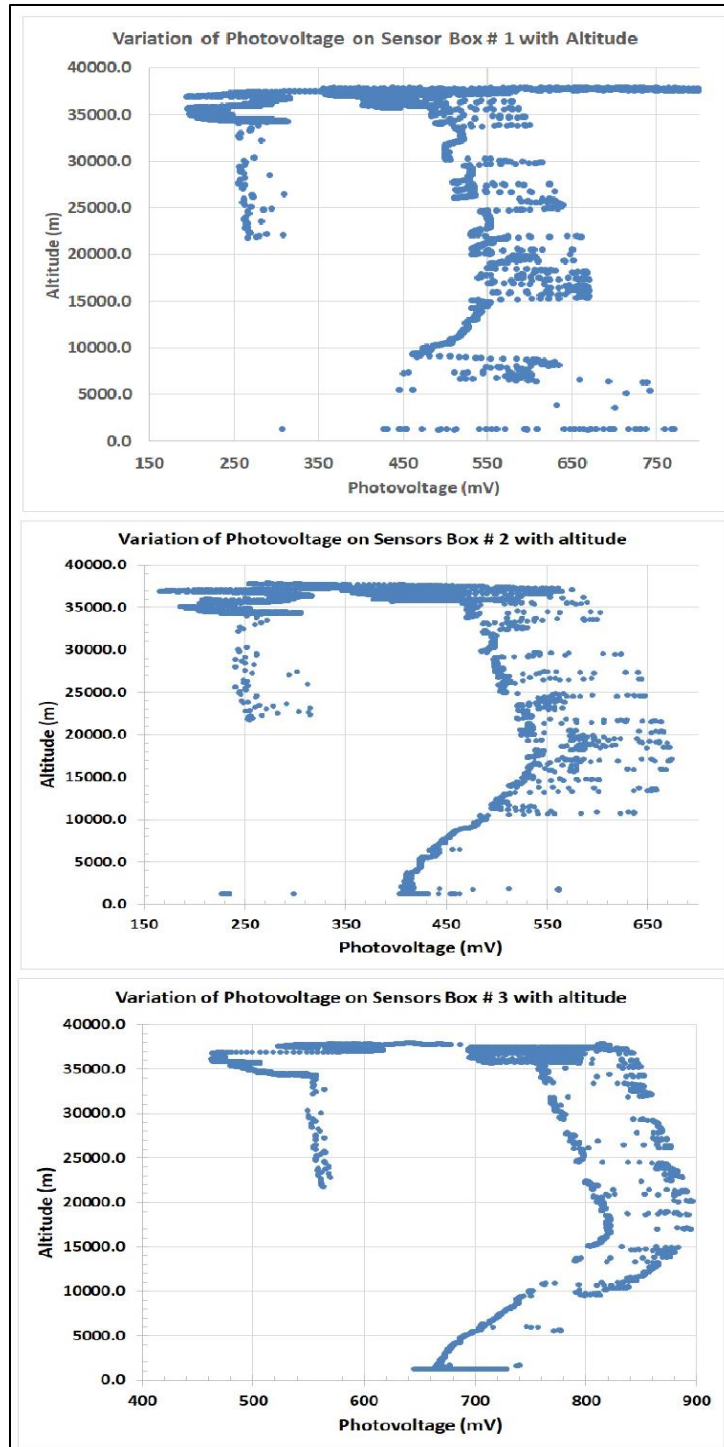


Fig. 1 (c) Response of UV light sensors mounted on sensors box#S1, S2 and S3.

The ozone profile measured by one of ozone sensors S1#8 during HASP 2021 flight is shown in fig. 1(d), while Ozone profile measured during HASP 2019 and HASP 2018 flight are shown in fig. 1 (e) and 1(d), respectively. Ozone concentration varied with altitude during each year.

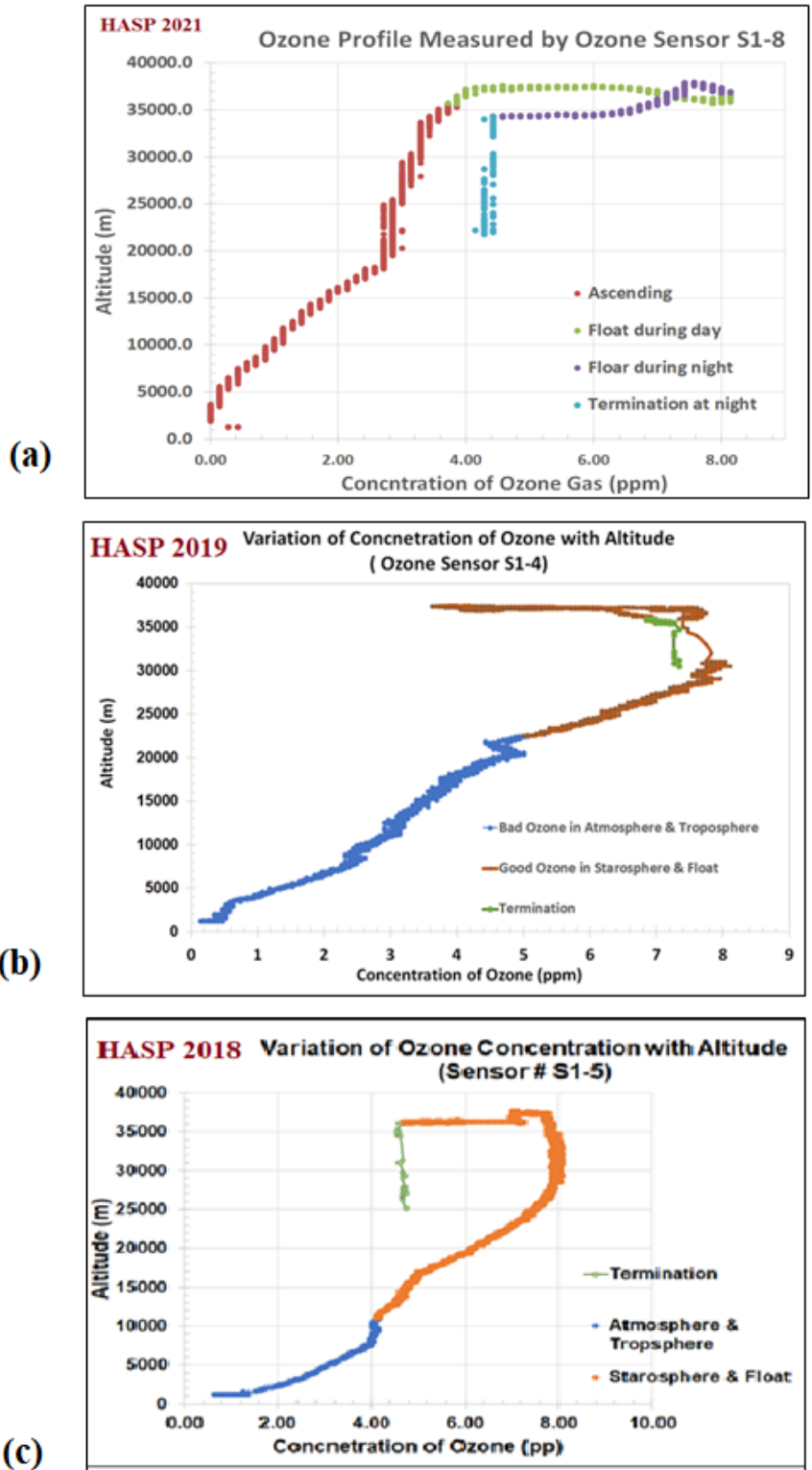


Fig. 1(a) Ozone profile measured by one of ozone sensor during **HASP2021** flight, (b) **HASP 2019** flight and (c) **HASP 2018** flight

1.1.3 Mission Objectives

Based on the success, few known technical problems and motivation with the HASP balloon flights made during previous flights, the UNF-UND team proposes a HASP 2022 flight with following new objectives for the measurement of ozone profile in the stratosphere using improved version of the gas sensors payload.

(i) Objectives of nanocrystalline thin film gas sensors boxes

Sensors Box #1

Improved version of nanocrystalline ITO thin film gas sensors array (Box#1) having better thermal stability and selectivity for detection of ozone gas.

Sensors Box #2

Use of stable alpha phase of silver tungstate (α - Ag_2WO_4) thin film gas sensors having better sensitivity for the measurement of ozone gas.

Sensors Box#3

New version of 8 nanocomposite based Al doped ZnO +ITO oxide semiconductor materials thin film gas sensors will be used for the measurement of bad ozone in pollutant gases and smog.

Students of UNF will fabricate ITO thin film gas sensors using an electron beam deposition method in Dr. Patel's research lab. Three sensors' boxes (#1, 2 and 3) will be mounted on the three sides of rectangular payload body.

We are interested to add Nano-ozone sensors having smaller in size for better performance by reducing number of grain boundaries. We are working on development and fabrication of Nano sensors using an Electron Beam Lithography (www.raith.com) attached with Scanning Electron Microscope (FEI, Quanta 200D). We may use Nano gas sensors in the 2022 flight if we are fully satisfied with performance of nano gas sensors in our laboratory.

All ozone gas sensors will be tested and calibrated simultaneously in the low-pressure chamber to minimize the experimental error for the determination of the trend line equations of the plots for converting the electrical resistance values into the concentration of ozone in the part per million (ppm). The pressure and temperature inside the test chamber will be maintained same as in the stratosphere for measurements of good ozone. Ozone sensors will also be tested and calibrated under troposphere and atmosphere conditions with an appropriate pressure and temperature ranges for measurements of bad ozone and nocturnal ozone.

(ii) UV light sensors

We will use all new GaP (FGAP71) UV light photodiode mounted below ozone sensor box. This UV light sensor will be maintained at constant temperature.

This GaP (FGAP71) photodiode has wavelength range 150 to 550 nm and peak wavelength of 440 nm, which is shown in Fig. 1(e).

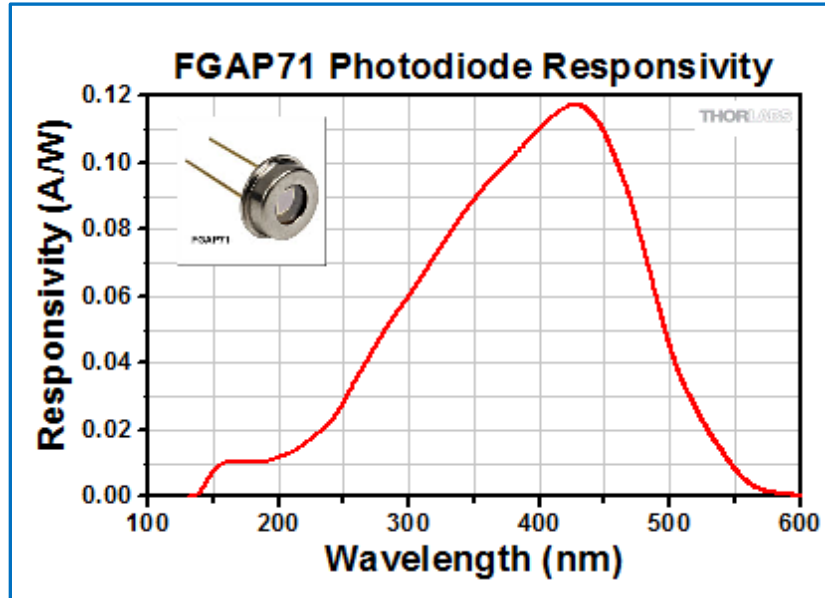


Fig. 1(e) Response of GaP (FGAP71) photodiode (Courtesy: www.thorlab.com)
http://www.thorlabs.com/newgrouppage9.cfm?objectgroup_id=285&pn=FGAP71.

Photodiode will be mounted just below the gas sensors box on each side of the payload body. The photodiodes will support the verification of science concept of generation of ozone in the presence of UV light. The amount of photo voltage generated and measured by the photodiodes will indicate how much of UV light available to interact with oxygen to convert into ozone gas near to ozone gas sensors. Our gas sensors arrays will detect and measure the concentration of that generated ozone gas. This **science concept** will also help us to understand the effect of any shadow or darkness on the sensors surface, particularly at the time of sunset and decrease of ozone concentration at the nighttime.

(iii) **New Low-Pressure Sensor**

It was observed that the pressure sensor used in the previous flight was worked from atmosphere to 100 mbar and then saturate. We propose to replace it by new pressure sensor, which can measure the pressure up to 10 mbar or below.

The new sensors may be purchased from

- (i) <http://www.meas-spec.com/product/Pressure/MS5540C.aspx> or
- (ii) (ii) <http://www.omega.com/pptst/PX170.html>

We need to adjust power and space to replace the new pressure sensor, otherwise, we will continue to use the same pressure sensors which we used in the previous payloads.

(iv) **GPS:**

The current UBLOX GPS worked well during last several flights and did not block at the high altitude. The antenna of GPS was installed away from the payload body and worked well. We will use the same GPS again. The payload GPS data will be cross verified and compared with the HASP GPS data.

(v) **Improved and thermally stable payload body:**

A single hollow aluminum tube structure will be used to make the payload body. The body work will be almost same as the last flight. This design will reduce the numbers of screws and nuts and hence weight of the payload. This will also allow us to open and close the payload easily for access of the hardware. We will try to reduce the mass of the body. The inner surface of body has very low outgassing at the low pressure and good reflections of Infrared light and heat. We are also exploring new alloy material as well as carbon fiber sheets to reduce the weight as well as improve the mechanical strength and thermal stability of the payload body.

Thermal blanket made of aluminized heat barrier having adhesive backed (Part No. 1828- or equivalent) (Make: www.PegasusAutoRacing.com) will be applied on the payload for the improvement of thermal stability. The silver surface of the thermal blanket has high reflection with wide range of wavelength of light and hence capable of withstanding radiant temperatures more than 1000°C as shown in Fig. 1(f). The payload covered with thermal blanket and ozone sensors maintained at constant temperature by the digital temperature controller make the sensors payload at isothermal condition for better thermal stability.

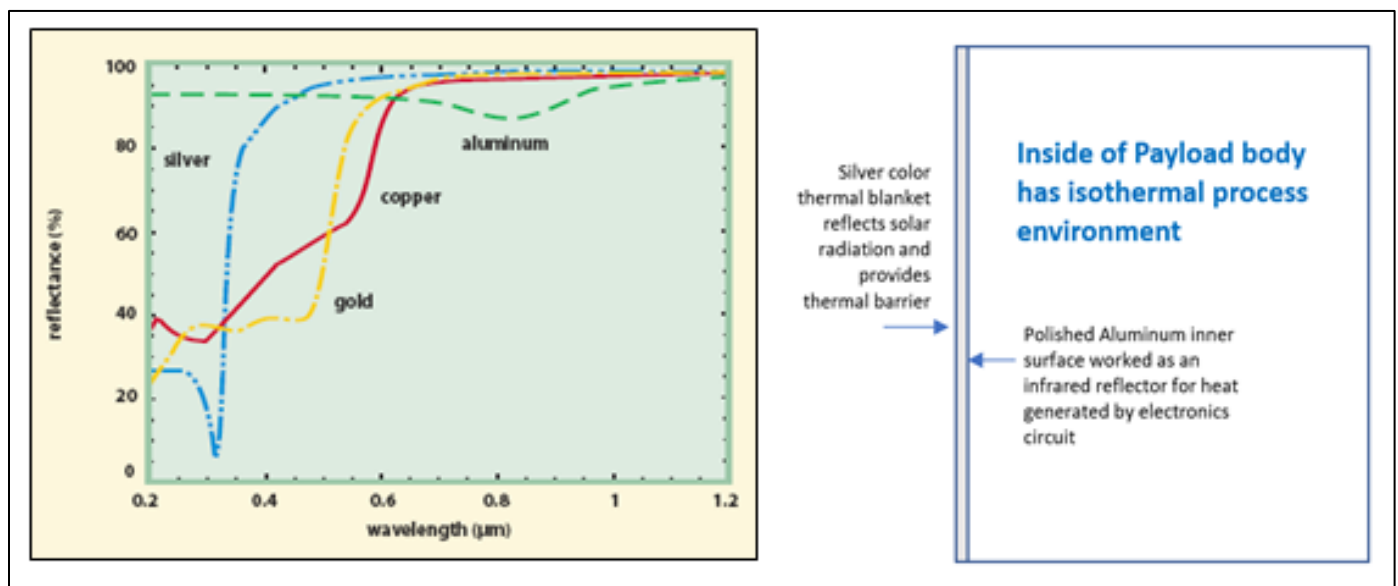


Fig.1 (f) Variation of reflectance with wavelength of light from different color of surfaces
Courtesy: <http://www.photonics.com/EDU/Handbook.aspx?AID=25501>

(vi) **Improved version of software**

New JAVA based software will allow us to convert all RAW files directly into one EXCEL file. Then, calibration trend line equations will be applied to convert the change in resistance values of sensors into the concentration of ozone gas in ppm. In addition, new LabVIEW program will allow us the quick monitoring of data and viewing of the plots during the thermal vacuum test and during the flight.

(vii) Use of SEM+EDAX

The surface topography of the sensors before and after the flight will be studied using a scanning electron microscope (SEM) (FEI, Quanta 200D), and the chemical composition of the surface of the sensors will be analyzed by energy dispersive analysis of x-rays (EDAX) at UNF under supervision of Dr. Patel.

(viii) Testing of the payload

Students will perform the electronic hardware and software testing of the payload at the UNF. They will also perform the mechanical tests including shock and stress analysis using simulation program. They will also perform the estimated thermal stability of PCB as well as sensors boxes at the low and high temperature under low and high vacuum in the vacuum chamber. All tests will be performed before integration of payload workshop at Palestine, TX. After flight, team will perform the failure analysis and data analysis and prepare the final science report.

(ix) Deliverable of HASP 2022

Working as a team, submission of monthly science report, participation of monthly videoconference, fabricate the working payload, testing and integration of payload with HASP at CSBF, Palestine, launching the payload and data collections, data analysis, and submitting the final science report.

1.2 Payload Systems and Principle of Operation

Nanocrystalline thin film gas sensors array will be fabricated over the ultrasonically and chemically cleaned glass substrates. The development of thin film of oxide semiconductor sensor was the part of three U.S. Patented sensors platform technologies invented by Dr. Patel at UNF [6-8]. Fig. 2(a) shows the top view of 8 sensor arrays and the interface printed circuit board. Fig. 2(b) shows a scanning electron micrograph of one ITO thin film gas sensor having two gold electrodes for the external electrical contacts. Fig.2(c) shows a scanning electron micrograph of nanocrystalline grains of the ITO thin film, while the sensor boxes are shown in fig. 2(d).

The payload will consist of three sensors boxes having three different types of gas sensors made by different materials.

Sensors Box #1

Improved version of nanocrystalline ITO thin film gas sensors array (Box#1) having better thermal stability and selectivity for detection of ozone gas.

Sensors Box #2

Use of stable alpha phase of silver tungstate (α -Ag₂WO₄) thin film gas sensors having better sensitivity for the measurement of ozone gas.

Sensors Box#3

New version of 8 nanocomposite based new oxide semiconductor Al doped ZnO+ITO materials thin film gas sensors will be used for the measurement of bad ozone in pollutant gases and smog.

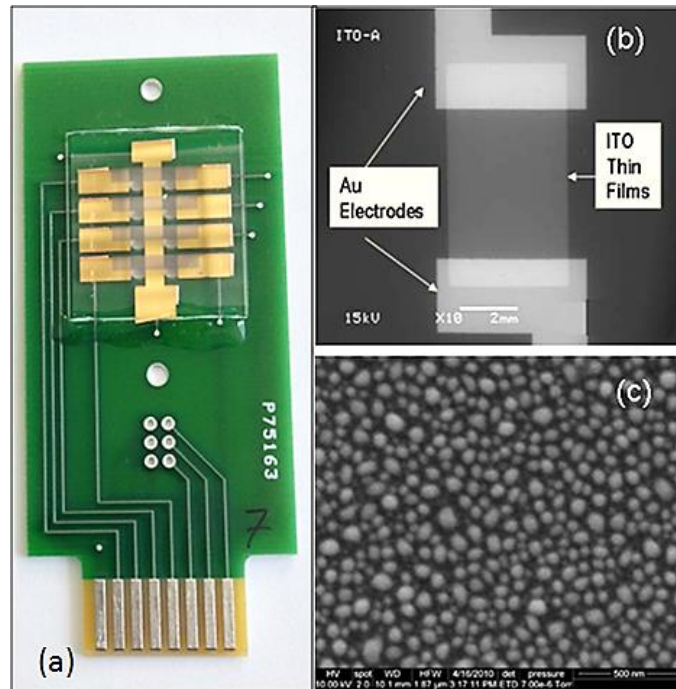


Fig.2 (a) 8 sensor array and interface mini-PCB, scanning electron micrograph of (b) top view of one ITO gas sensor, and (c) nanocrystalline grains of ITO thin film

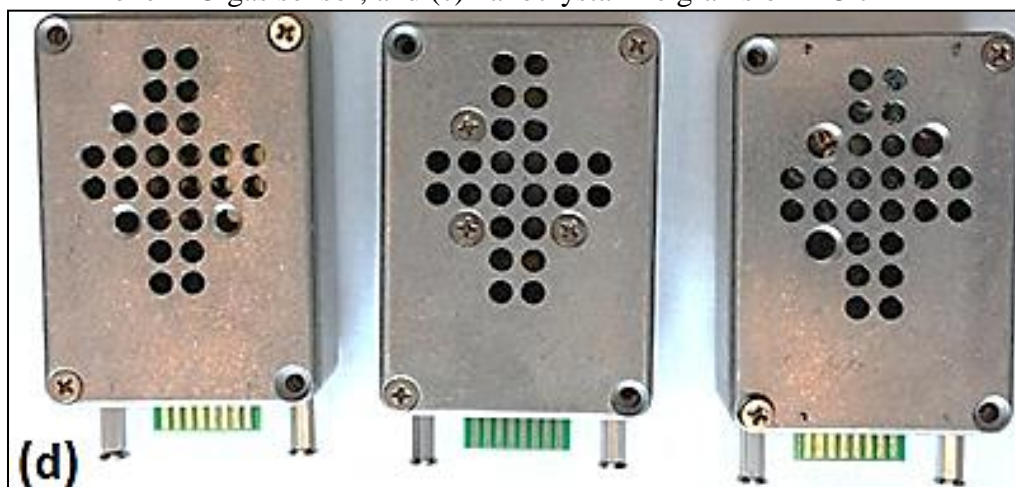


Fig.2 (d) sensors boxes

Each type of sensor array box will have different sensor characteristic parameters for the detection of gases. Three different types of gas sensor arrays boxes will be fabricated at UNF.

Fig. 3 (a) shows the picture of housing for the UNF sensors, consisting of an array of 8 gas sensors interfaced with a printed circuit board (PCB), flexible Kapton heater (MINCO make HK 5573R30.0 L12BU), temperature sensor (Analog Device TMP36), electrical fan (SUNON, MC25060V2-0000-A99, DC 5V, 0.38W) and a 16 wires flat cable. One end of flat cable has a female card edge connector to connect sensor PCB (Make 3M, MCS16K-ND), while another end has 16 pins female to connect microcontroller PCB.

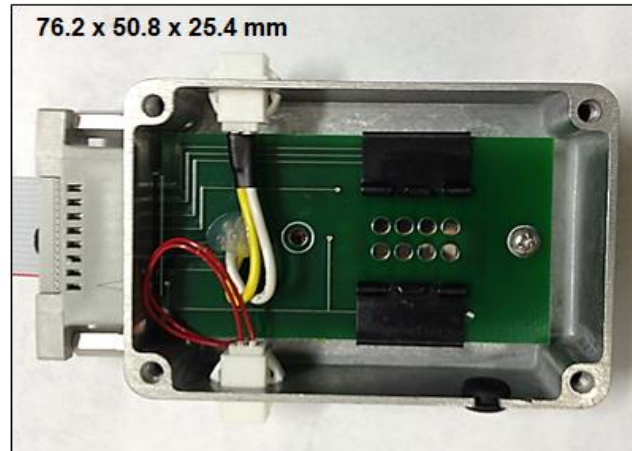


Fig. 3(a) the picture of sensors box of the payload. The sensor box consists of 8 ozone sensors array mounted on the PCB with one heater, miniature fan, and a temperature sensor.

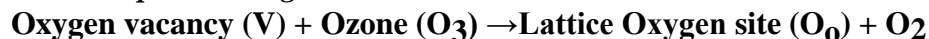
The sensor array will be interfaced with the printed circuit board and its 16-pin female card edge connector and flat cable. Sensors will be tested and calibrated with ozone under low pressure at UNF. An ozone generator (Ozone Solutions, Model# OMZ-3400) will be used as the source of ozone, which generates 0 to 12 ppm ozone gas. A digital ozone detector (Eco Sensors, Inc., Model:A-21ZX) will be used to measure the concentration of ozone. Keithley electrometer and multimeter with LabVIEW software will be used to measure resistance of all sensors simultaneously in the test chamber. The parameters of trendline equations of calibration plots will be used for the determination of concentration of ozone.

Working Principle of Gas Sensors

Interaction of oxidizing gas on surface of n-type ITO thin film sensor

Upon adsorption of charge accepting molecules at the vacancy sites, namely from oxidizing gases such as ozone (O₃), these electrons are effectively depleted from the conduction band of ITO. This leads to an increase in the electrical resistance of n-type ITO.

For example: ozone gas:

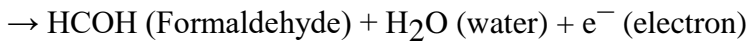
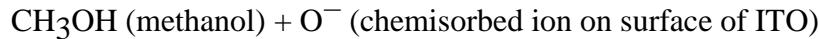


Vacancies can be filled by the reaction with ozone. Filled vacancies are effectively electron traps and consequently the resistance of the sensor increases upon reaction with ozone.

Interaction of reducing gas on surface of n-type ITO thin film sensor

Oxygen vacancies on ITO surfaces are electrically and chemically active. These vacancies function as n-type donors decreasing the electrical resistivity of ITO. Reducing gases such as CO, H₂ and alcohol vapors result in detectable decreases in the electrical resistance of n-type ITO.

For example: methanol:



Vapors encounter the surface and react with chemisorbed oxygen ions O⁻ or O²⁻ and re-inject electrons into the conduction band.

In summary, the electrical resistance of ITO increases in the presence of oxidizing gases such as ozone. Upon adsorption of the charge accepting molecules at the vacancy sites, namely oxidizing gases such as ozone, electrons are effectively depleted from the conduction band, leading to an increase in the electrical resistance of n-type ITO. Note that our three different types of sensors boxes have n-type semiconductor gas sensors.

Steps for Measurements of Ozone

Fig. 3(b) shows various steps for the detection of ozone by the sensors payload during the flight. The detection of reducing gases will also have similar steps. Team has also developed the program for testing the HASP payload. The different style of screens for quick monitoring data directly from the LSU website server can be possible. This LabVIEW based program will save time to download the files and then apply software program to put data in EXCEL and then make plots. This will help us monitoring data easily during the thermal vacuum test as well as during the flight.

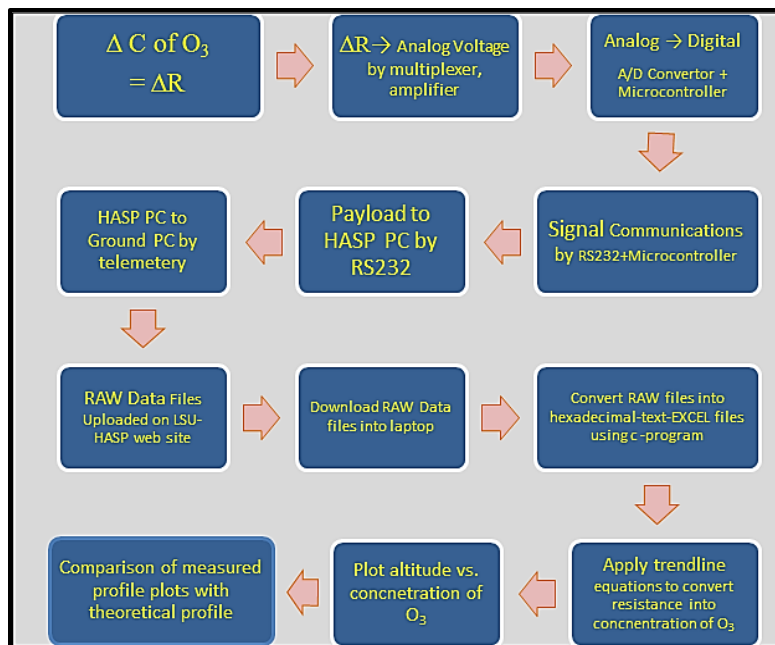


Fig. 3(b) Steps for the detection of ozone by the payload

1.3 Major System components

The payload will consist of three sensors boxes. Each sensors box will have 8 gas sensors, 1 flexible heater, 1 temperature sensor and 1 mini fan. Three sensors' boxes will be mounted on three side of cubic payload body. Gas molecules can enter in the sensor box through perforated holes on the payload body. Fan will protect the surface of sensor by blowing away dust particles in the atmosphere and ice particles in the troposphere. Temperature of ozone gas sensors will be maintained nearly constant at about $305 \pm 5^\circ$ K using the temperature controller. Flexible heater (MINCO or OMEGA make) and temperature sensor (Analog Device TMP 36) will be mounted on the back side of gas sensors. All gas sensors, UV light sensors, GPS, pressure sensors, temperature sensors will be interfaced with a microcontroller circuit board.

1.4 Mechanical and Structural Design

The important features of our newly designed payload body are easy to open and close the payload, easy access of PCB and sensor boxes, low rate of outgassing under low pressure, better stability with thermal and impact, and reusable. The payload metal parts were procured payload from the supplier www.onlinemetals.com.

We are interested to replace a square aluminum tube by a fiber glass or carbon composite square tube to reduce the weight of payload and improve the thermal stability. We may order the fiber glass tube from <http://www.eplastics.com/Fiberglass-FRP-Round-Square-Tubing>. Currently, this company has short supply of 6-inch square tube.

The payload has easy to open and close design utilizing the top plate for access to the PCB as well as all sensor boxes. The payload continues to feature a rectangular design due to its robustness as well as for its low rate of outgassing under extreme pressure drops. This design is optimal for the team's goal of a reusable payload body. The details of design and drawing and fabrication work are shown in fig.4 (a) to (u). The design of proposed payload will be same as design made by Corrina Yorke (HASP2018) using AutoCAD. UNF students will perform fabrication work of the payload body in the UNF workshop. The outer dimensions of payload body will be about 228.6 mm height, 152.4 mm depth and 152.4 mm width.

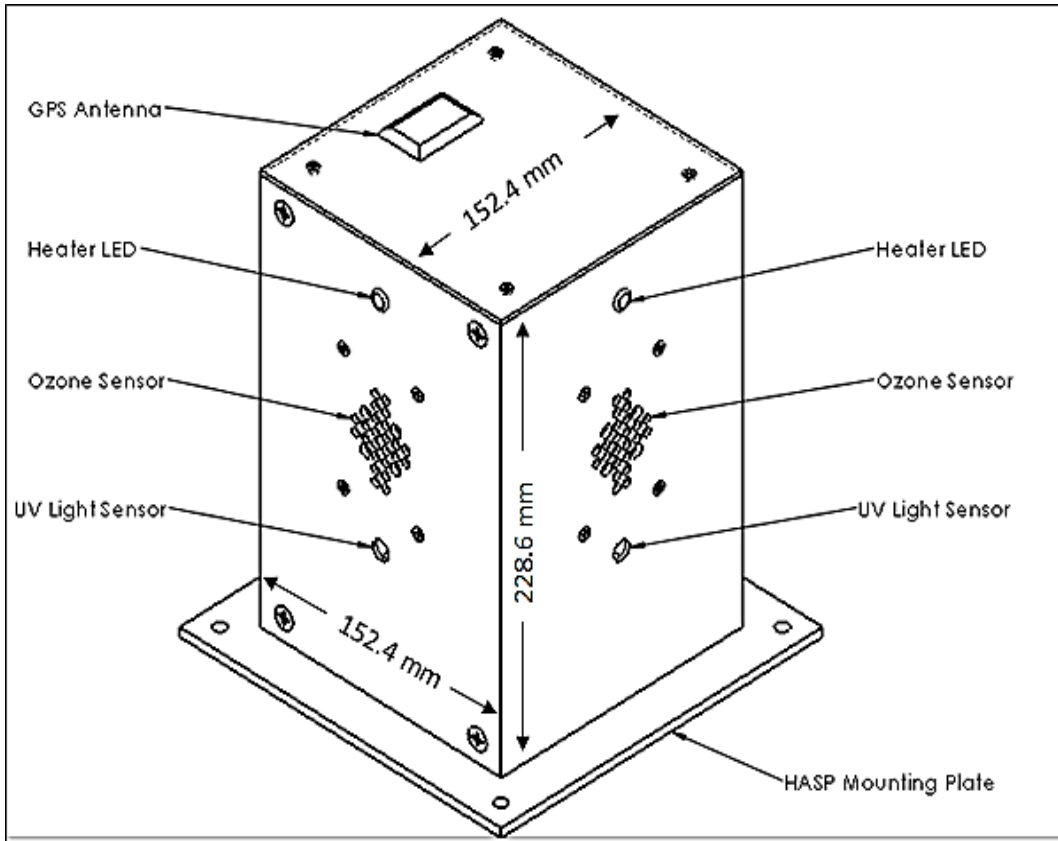


Fig.4 (a) Design of payload body.

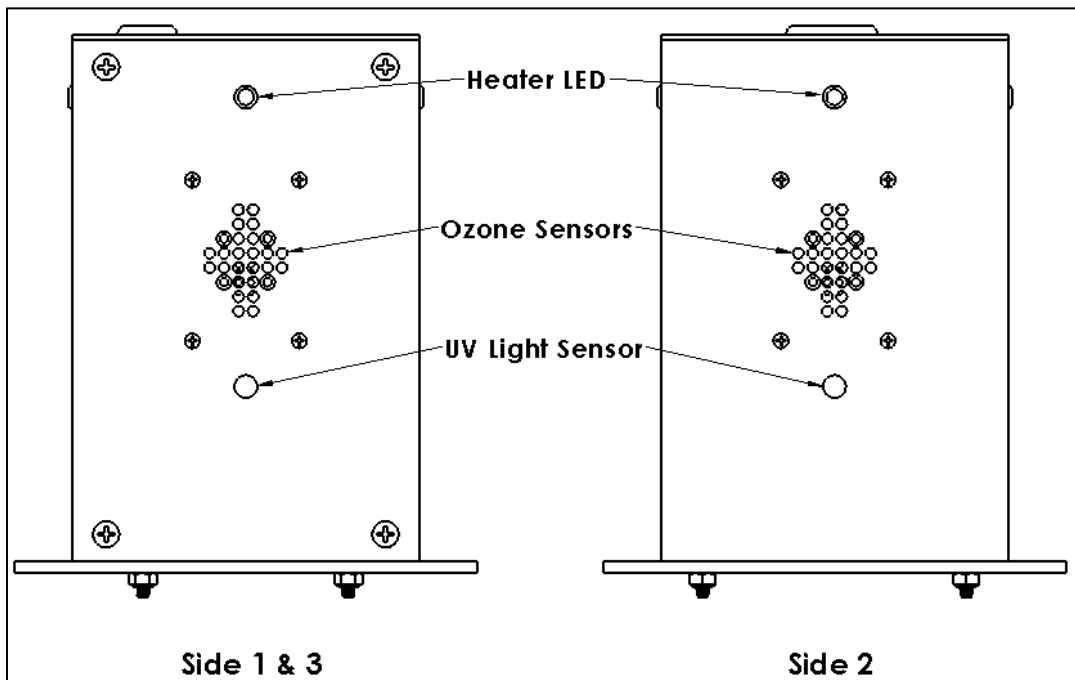


Fig. 4 (b) Side view design of the payload

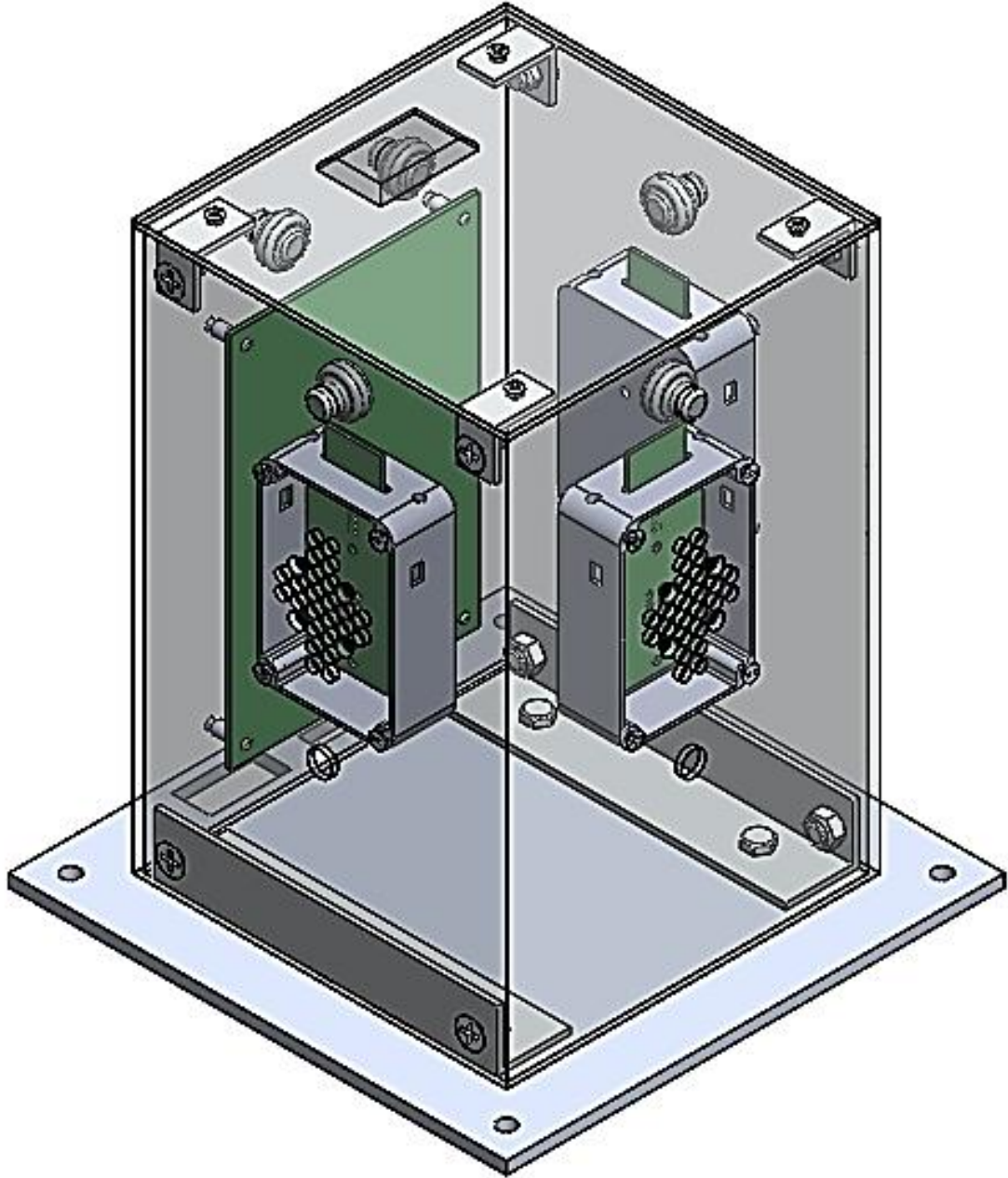


Fig. 4 (c) Design of all sides' view of the payload mounted on the HASP plate.

The payload was mounted on the HASP mounting plate using aluminum L-brackets, bolts, washers, and nuts. We will make sure, that the payload will be well secured so that it remains intact and attached to the HASP mounting plate under a 10 g vertical and 5 g horizontal shock. In addition, the payload body is aluminum so that it will certainly survive and operate in the very low-pressure range of 5 to 10 millibars at the float altitude.

The additional details of mechanical drawings are given in fig. 4(d) to 4(v) of Appendix-A.

Payload Mounting Footprint

Selection of the small payload dictates the mounting plate that interfaces with the payload. This mounting plate design is provided in the HASP Student Payload Interface Manual (Version 02.17.09) and is shown below in Fig.5. This mounting plate design will not require any modification except to make four mounting holes as shown in fig. 5.

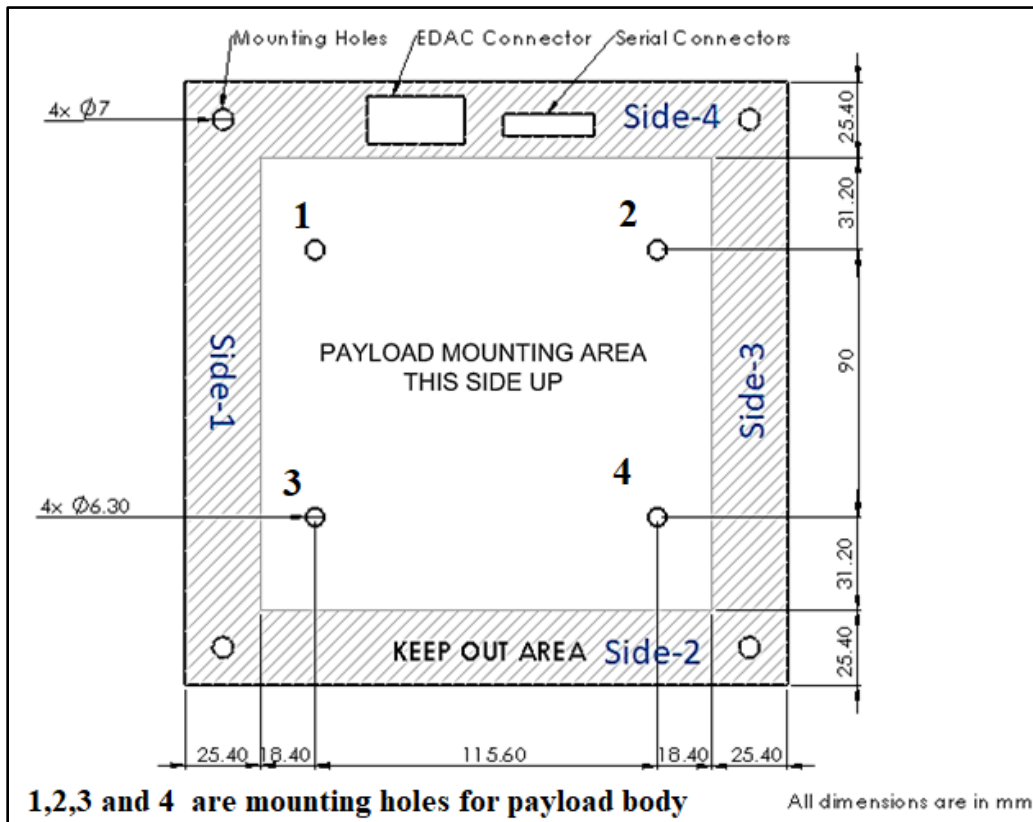


Fig. 5 Mounting Plate for small payload (Courtesy: HASP Version 02.17.09 [9])
http://lasp.space.lsu.edu/hasp/documents/public/HASP_Interface_Manual_v21709.pdf

1.5 Electrical Design

The block diagram of circuit is shown in fig. 6 (a).

Several sections of circuits diagrams are given in Appendix-B. Refer fig. 6 (b) to (j) for additional details of circuits. Two identical microcontroller PCBs will be fabricated. One PCB will be used for the payload, while for other PCB will be used to stimulate software and backup.

The microcontroller circuit was designed by Jonathan earlier and then redesigned and refabricated by Ken, Brittany and Chris.

Please excuse us for smaller and lighter fonts in the circuit diagram. We will modify it in larger fonts size later on.

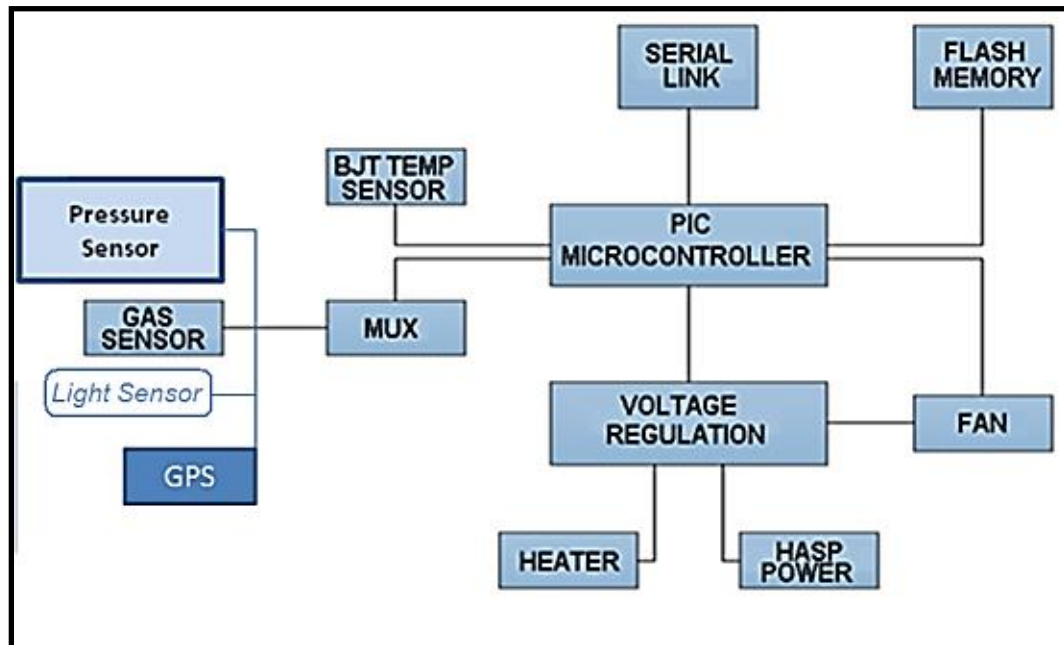


Fig. 6(a) Block diagram of payload circuit

1.6 Thermal Control Plan

Preliminary heat transfer calculations using equation (1), heat transfer, showed the onboard sensor heater is adequate to keep the sensor at the nominal conditions. An additional exploration of the effects of temperature on component integrity is ongoing, and part of the investigation. These initial estimations utilized the proposed materials for the walls, and a minimum temperature of -60°C ($=333\text{ K}$ or 140°F) and a general operating temperature of 15°C ($=288\text{ K}$ or 59°F) (found from altitude variation from 0 km to 36 km shown in the modified altitude profile (Fig. 7).

$$\text{Heat Transfer} = q = m(\Delta T) C_p \quad (1)$$

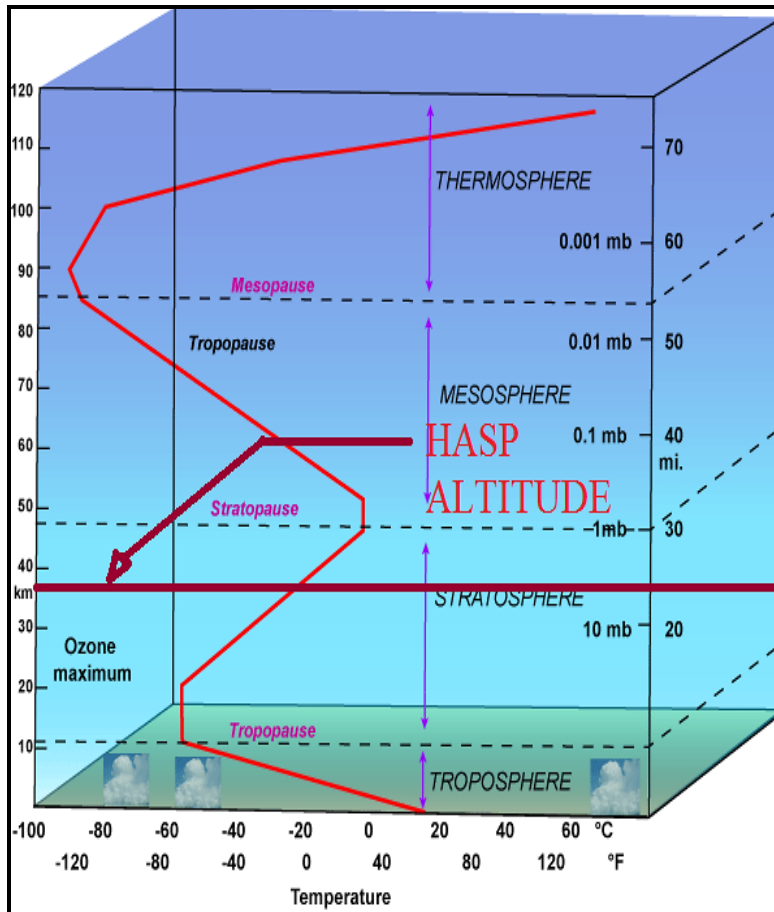


Fig. 7 Modified Altitude Profile by Atkins [10]

Our previous payload had good thermal stability. The payload body has better thermal stability against conduction and convection of heat from temperature range $-50\text{ }^{\circ}\text{C}$ to $70\text{ }^{\circ}\text{C}$ under high as well as very low-pressure conditions. We will try to further improve the thermal stability of the payload. As mentioned in our objectives, the outer surface of payload body will be covered by the thermal blanket made of aluminized heat barrier having adhesive backed (Part No. 1828) (Make: www.PegasusAutoRacing.com) for the improvement of thermal stability. The high reflective surface of the material can withstand radiant temperatures more than 1000°C . This thermal blanket will minimize the variation of internal electronics temperature conditions. The temperature of ozone sensors will be controlled in the range of $302 \pm 6^{\circ}\text{K}$ using an On-Off controller, a polyimide flexible heater (MINCO make) and a temperature sensor TMP 36). We may replace the aluminum body of payload by fiber glass or carbon composite or alloy body for reducing weight as well as improving thermal stability.

The variation of temperature of three ozone sensors boxes #1, 2 and 3 with altitude during the HASP 2021 flight is shown in fig.8(a) for information. The temperature of sensors was remaining constant $303 \pm 6^{\circ}\text{K}$. The variation of temperature of ozone sensors in box#1, 2 and 3 with time (UTC) is shown in fig. 8 (b).

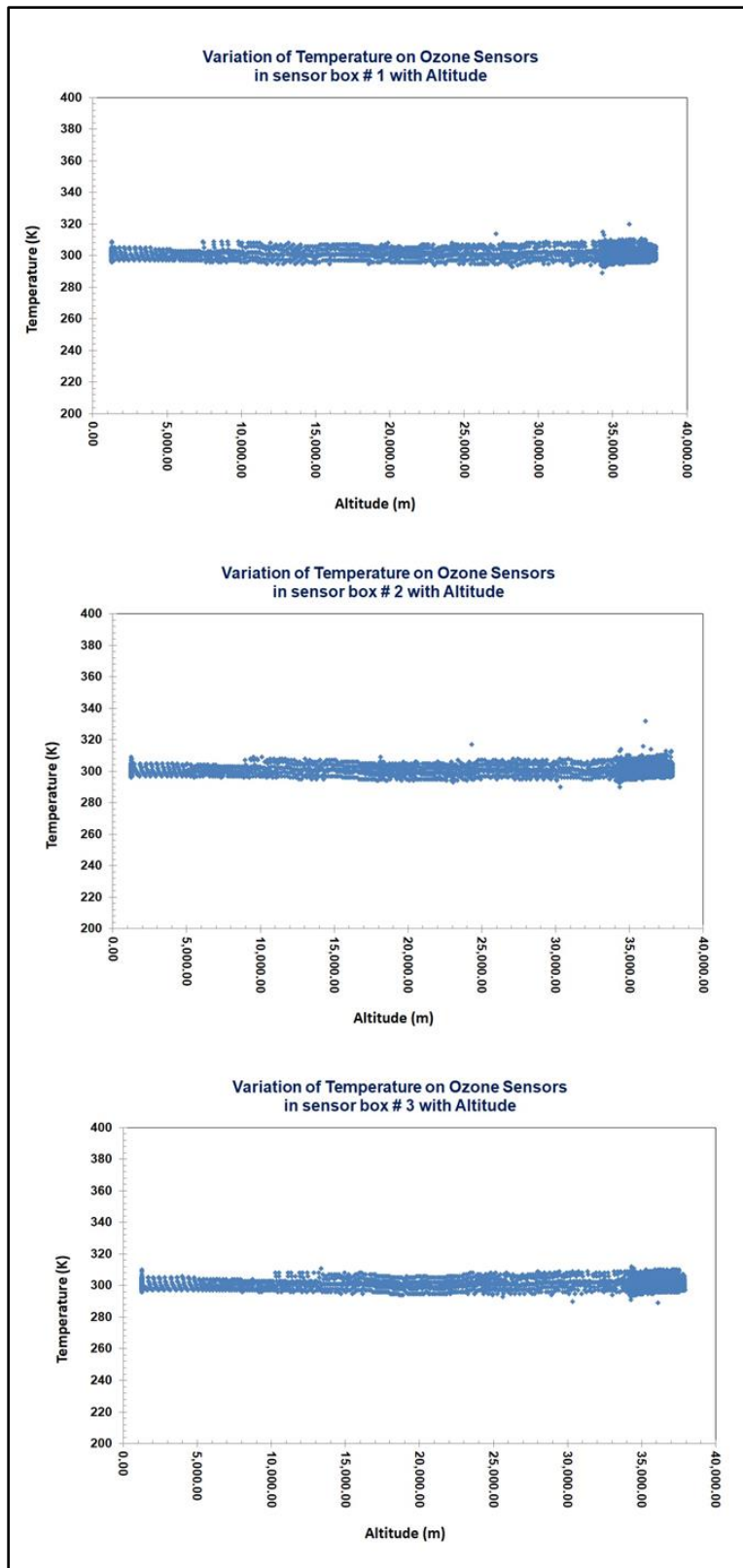


Fig. 8 (a) Temperature of ozone sensors box#1, 2 and 3 during HASP 2021 flight.

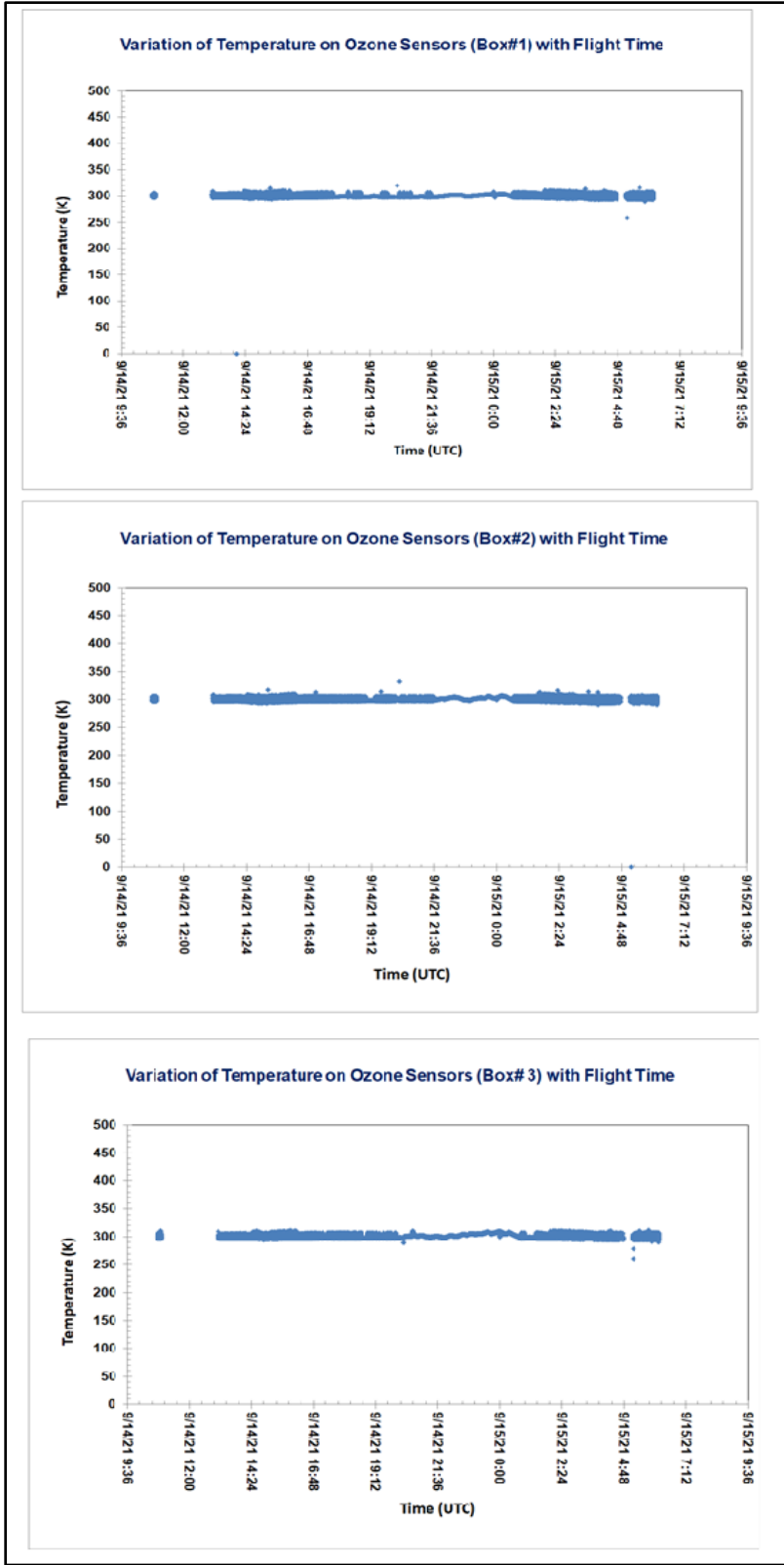


Fig.8 (b) Variation of temperature of ozone sensors in box#1, 2 and 3 with time (UTC) during HASP2021 flight.

2. Team Structure and Management

2.1 Team Organization and Roles

Fig.9 shows the chart for the team management. The listed work distribution is tentative, which will be organized further after making first Zoom video conference in January 2022.

HASP 2022	
UNF	UND
Dr. Nirmal Patel UNF Faculty Advisor	Dr. Ron Fevig UND Faculty Advisor
Miguel Bolante (Team Leader) Administration, reporting, meeting, PCB, hardware, and sensors fabrication. Electrical, weight, and power budget and thermal control	One UND Student will join later.
Michael Shearer Atmospheric Chemistry, Sensor materials, Fabrication of sensors. Testing and calibration of sensors.	
Diego Fontan-Ulibarri Payload body design, fabrication and integration.	
Karli Dattilo Software, Programming, Payload testing and Data Analysis.	
One EE/CE student Helping Miguel for Microcontroller Circuits and Testing work and Karli for Programing work.	

Fig.9 UNF-UND team

Faculty Advisors

Both Dr. Nirmal Patel (Faculty Advisor from UNF) and Dr. Ron Fevig (Faculty Advisor from UND) are involving in the development of sensors payload and participated HASP balloon flight since 2008. Both were jointly conducted teleconference, FaceTime conference on cell phones, text messages, email communications with their team members regularly every month for the previous flights. This will be continuing for HASP 2022 too. Dr. Patel is mentoring students for the fabrication, testing and calibrations of nanocrystalline gas sensors, design and fabrication of payload, data analysis and improvement of software program, while Dr. Fevig is mentoring students for the improvement of microcontroller circuits, interfacing of sensors, atmospheric studies, and space applications. Both Dr. Patel and Dr. Fevig are citizen of USA.

Demographic Information of Students

Miguel, Karli, and Diego worked as team members during last HASP 2021 flight and will continue to work for HASP 2022. All team members are citizen of USA. Miguel Bolante is a dynamic Electrical Engineering student. He studied under Dr. Patel. He will continue to work as a team leader. He will take on organizing the meetings, zoom video conference meetings with all members and faculty advisors and communicating with the HASP. He will take lead for the integration and thermal vacuum testing of payload at Palestine, TX and pre-flight testing at Fort Sumner, NM. He will also be responsible for the flight operation plan, monthly reports, travels, and updating of progress of work and any issue to both the advisors and for the final science report. The demographic information of all students is given in table 1.

Table-1 Demographic information of students

#	Name	Gender	Ethnicity	Race	Student Status	Disability
University of North Florida Students Team						
1	Miguel Bolante (Leader) Phone 904-482-3673 m01434191@unf.edu	Male	Hispanic	Caucasian/White	UG-EE	No
2	Michael Shearer Phone 904-524-5199 N01066573@unf.edu	Male	Non-Hispanic	Caucasian/White	PG-Materials - ME	No
3	Karli Dattilo Phone: 904-729-6757 N01430516@unf.edu	Female	Non-Hispanic	Caucasian/White	UG-CE	No
4	Diego Fontan-Ulibarri Phone 321-614-1632 N01420752@unf.edu	Male	Hispanic	Caucasian/White	UG-CE	No

2.2 Timeline and Milestones

The initial work breaks down schedule includes the basic tasks required of the HASP project, which includes the Proposal, Integration Plan, Integration Certification, Operation Plan, and Science Report. The proposed work plan path is given in table.

Table-2 Timeline and Milestones

2022	UNF	UND
January	Conceptual Design Review (CoDR) for sensors, electronic circuits, software, and payload. Reviewing science reports and issues of HASP2008 to 2021 flights.	
February	Preliminary Design Review (PDR) for sensors, electronic circuits, software, payload, integration of payload with HASP and data analysis.	
March	Critical Design Review (CDR) for sensors, electronic circuits, software, payload, integration of payload with HASP and data analysis.	
April	Designing of circuit board and programming. Fabrication and testing of sensor arrays, designing of payload body	
May	Fabrication of circuit board and programming, modifications, if any Calibration of sensors and delivery of sensor arrays to UND for testing. Complete Payload Specification and Integration Plan (PSIP).	
June	Fabrication of sensors box and payload body. Reviewing HASP flights, data, and any issues.	Testing of circuit and sensor arrays. Integrating the circuits and the sensor arrays.
July	Integration of circuit board and sensor box with the payload body. Development of protocols for communication of payload with HASP computer and RAW files to EXCEL file Integration of sensor arrays in box. Integration of sensor boxes with payload body. Integration of PCB to payload and sensors box.	
August	Performing several tests on the payload at UNF. Flight operation plan, Testing payload, thermal vacuum test of payload and integration of payload with HASP platform. Submit Flight Operation Plane (FLOP)	
September	Pre-flight testing of payload, launching of payload and downloading data files, and data analysis work	
October	Payload recovery, testing of sensor arrays and other components, SEM+EDAX analysis of sensor arrays and finding of issues and performing failure analysis. Completing Data analysis.	
November	Data analysis and writing the final science report.	
December	Submission of the science report and planning for the next flight.	

Every month

- **First Friday – To attend HASP Zoom Videoconference.**
- **Last Friday-To submit the monthly status report.**

2.3 Anticipated Participation in Integration and Launch Operations

It is expected that at least three students from UNF, one or two students from UND and Dr. Nirmal Patel, faculty advisor from UNF will travel to CSBF, Palestine, Texas during the dates given by HASP for the integration of the sensor payload onto HASP. It is also expected that approximately two students from UNF and UND and one faculty member (UNF or UND) will travel to Ft. Sumner, NM for launch of the HASP2022 payload during the dates given by HASP and CSBF.

Anticipated Procedures

Prior to Integration:

- Testing and Calibration of sensor arrays
- Set initial values for data recorder
- Place sensor arrays in appropriate payload slots
- Check program and LED for status

Integration:

- Mount payload module to HASP
- Connect HASP Power Connector as shown in Fig 10
- Connect HASP Serial Connection as shown in Fig 10



Fig. 10 Connection of power and data communication cables of HASP with the payload (#7).

- Test system by recording initial readings and making sure all data is nominal
- Troubleshoot

List all checks that will determine a successful integration:

- Perform communication and data checks.
- Successfully execute command set.
- Monitor system to ensure proper operation via real time data stream of all sensors data readings, pressure, photo voltage of light sensors and ambient temperature.

Pre-Flight Operations and testing:

- Set initial values for data recorder
- Place sensors in appropriate payload slots
- Remove the protecting cover from the payload body
- Connect HASP Power Connector
- Connect HASP Serial Connection
- Check mass and size of payload
- Test thermal-low temperature and high temperature test and all commands
- Test pressure and vacuum test
- Test 10g vertical and 3g horizontal vibration/impact test

Duration of Flight:

- We are flexible for the duration of flight. Minimum 6 to 8 hours' flight during **daytime** will be fine for us.

Flight Operations:

- Record values for resistance across the sensors

Post-Flight Operations:

- Examine all parts of payload. Test working of the payload.
- Remove PCB and sensors box from the payload. Test PCB with power and test sensor box
- Examine sensors box for electrical testing, SEM+EDAX analysis, and determine failure analysis, if any.

3. Payload Interface Specifications

3.1 Weight Budget

The estimated weight budget of various parts of the payload is given in the table 3.

Table-3 Payload weight and dimension budget

Item:	Dimension	Mass ± Uncertainty (g)
8 Ozone sensors box #1 (including fan, heater, box)	Each box 3 x 2 x 1 inch	200.0±2.0
8 Ozone sensors box #2 (including fan, heater, box)	=76.2x50.8x25.4 mm	200.0±2.0
8 Pollutant sensors box#3 (including fan, heater, box)		200.0±2.0
Microcontroller PCB with mounted components	4x 6 inch =101.6 x152.4 mm	300.0±1.0
Payload body, top plate, and thermal blanket	9 x 6 x 6 inch =228.6x152.4x152.4 mm	1000±10.0 g
Few Cables, 1 GPS, 2 LEDs, 3 Photodiodes, nuts, and bolts		300±5.0 g
HASP mounting plate	7.9 x 7.9 inch =200.6x200.6 mm	550±3.0 g
Total estimated mass of the payload with HASP mounting plate		2750±12 g

3.2 Power Budget

As per the instructions, on the EDAC 516 power connector only pins A, B, C, D are wired to the payload as +30 VDC power supply and pins W, T, U, X are wired to payload as power ground to avoid failure to the power circuit or loss of payload. A voltage regulator is not necessary according to initial tests despite the slightly higher +33 VDC at launch for the sensor; however, a voltage regulator and divider will be used for peripherals. Fig. 11 (a) shows the EDAC516 receptacle pin layout.

HASP will provide power to our payload through EDAC516 connector. The following fig. 11 (b) shows the circuit diagram for interfacing of HASP mounting plate EDAC516 connector with voltage regulation of payload subsystems. Below is the switching power supply circuit, which is used in previous payloads. It has performed flawlessly. It is based around a National Semiconductor LM2956-3.3 switcher with ramp up voltage capability provided by C11, R13, and R14. 30 volts from the EDAC connector is provided via its 4 connections to a reverse protection diode, D11. A current limiting resistor, R1, is in series with D11. The 30-volt supply is then reduced to 3.3 volts via the switching power supply U21 and supporting components.

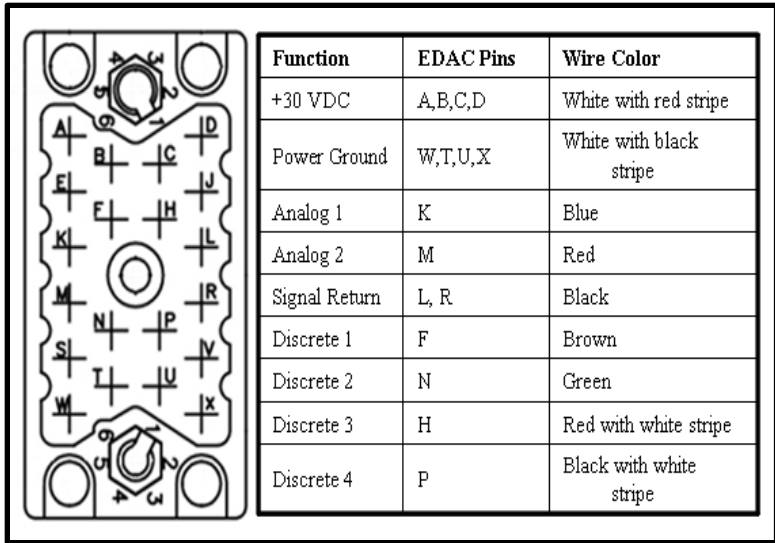


Fig. 11(a) EDAC516 receptacle pin layout (Courtesy: HASP manual).

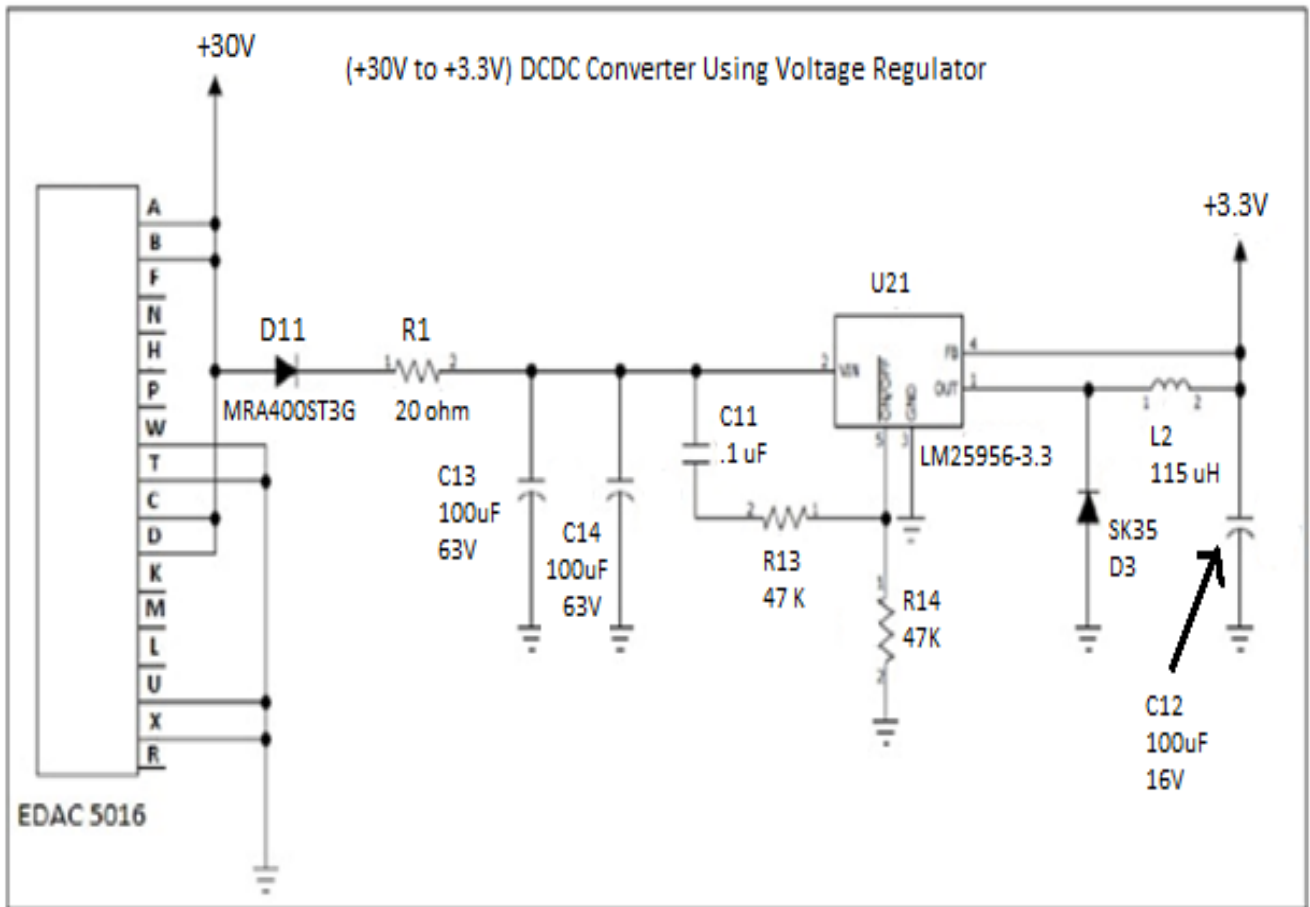


Fig. 11 (b) interfacing of EDAC 5016 of mounting plate with the payload voltage regulation circuit.

The voltage applied to the payload during the HASP 2021 flight is shown in fig.12 (a) for information. It was found that applied voltage remains nearly constant about 3300 mV.

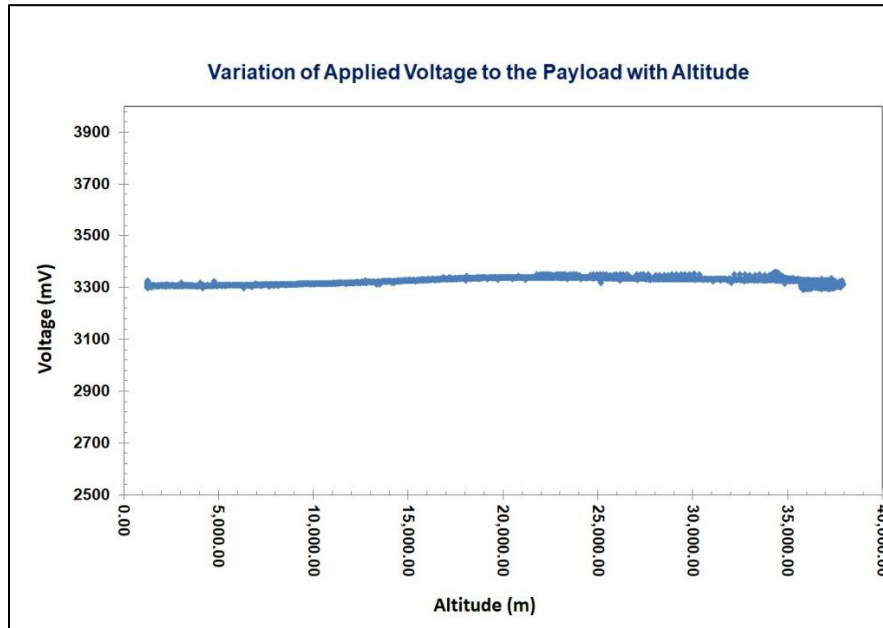


Fig.12 (a) Voltage applied to the payload during the HASP 2021 flight.

The current drawn by the payload during the HASP 2021 flight is shown in fig. 12(b). The current drawn by the payload during the flight was

Measured current drawn by the payload during HASP 2021 flight at 3.3 VDC for different function of circuit operation is listed in the table 4.

Table-4 Current Draw by the payload during HASP 2021 flight

Circuit Function	Current draw (mA)
Payload Power ON, but all heaters OFF	35±6
Payload Power ON and Heater #1 ON	140±12
Payload Power ON, Heater #1 and 2 ON	260±14
Payload Power ON, Heater #1, 2 and 3 ON	360±15

The power budget was maintained under the upper limit of HASP requirement during the previous HASP 2021 flight.

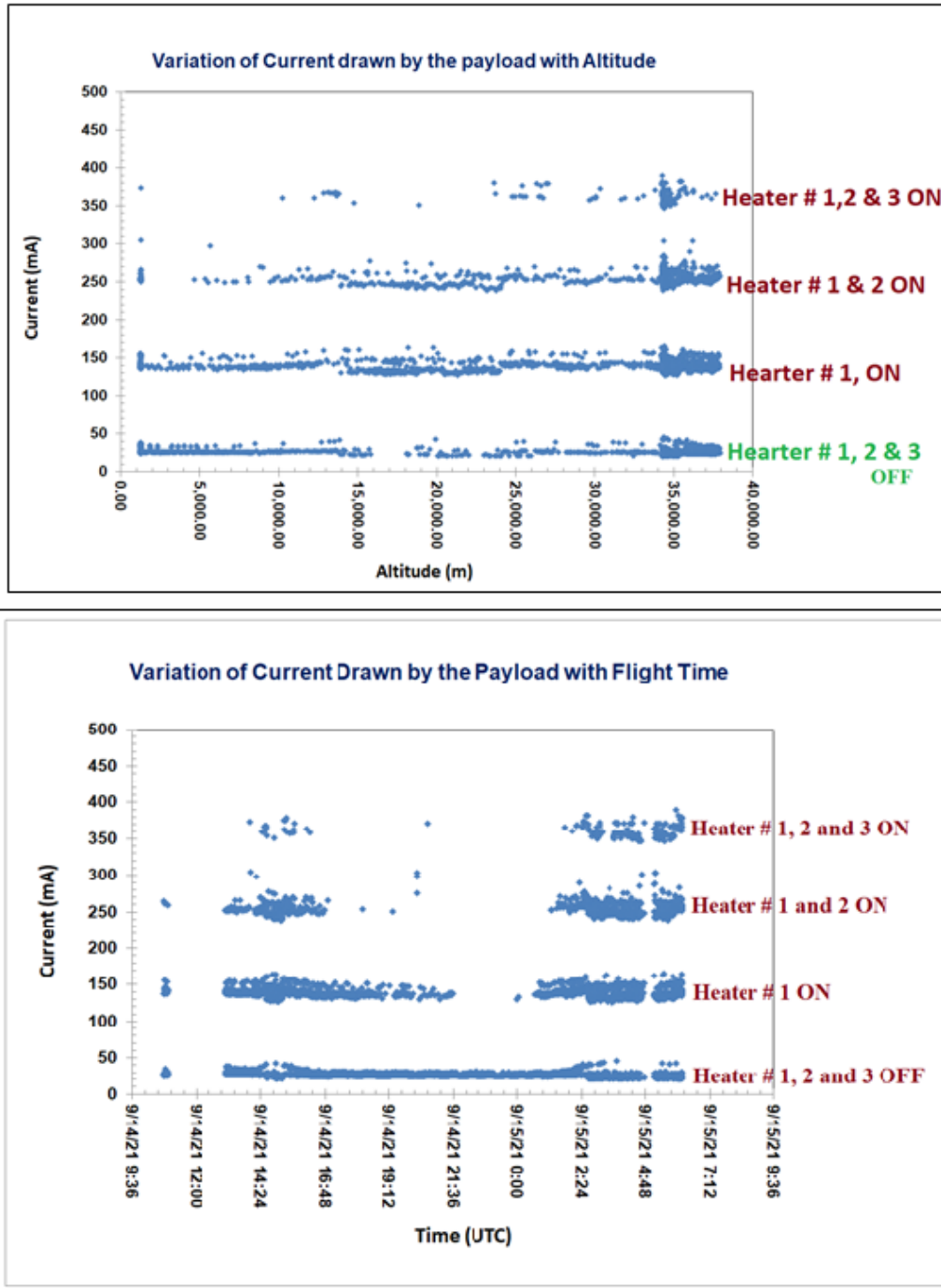


Fig.12 (b) Current drawn by the payload during the HASP 2021 flight

The 0.5Amps at 30VDC power supplied by HASP adequately accommodates the power requirements for the payload electronics, as well as the heater and fan for the sensor. The expected current and power drawn by the payload at 3.3V applied voltage are given in the following table 5.

Table-5 Expected Power budget of the payload for HASP 2022

Circuit Function	Current draw (mA) at 3.3 V	Power (W) Draw at 3.3 V
Payload Power ON, but all heaters OFF	35±6	0.12±0.02
Payload Power ON and Heater #1 ON	140±12	0.46±0.04
Payload Power ON, Heater #1 and 2 ON	260±14	0.86±0.05
Payload Power ON, Heater #1, 2 and 3 ON	360±15	1.20±0.05

The minimum power drawn by the payload will be about 0.12 ± 0.02 W, while maximum power drawn will be about 1.20 ± 0.05 W. Most of time power drawn by the payload during the float will be less than 1.0 W. This expected power consumption is less than the 15 W limits for the smaller payloads.

3.3 Downlink Serial Data

The payload module requires the RS232 HASP telemetry to send the status of resistance values to the ground. A data-recording unit will be included with master controller on PCB if the telemetry link fails. The DB9 connector (Fig.13) is required to the HASP system's telemetry system so that the data can be sent to the base station via the RS232 link. The RS232 link will operate at 2400 baud, with the standard RS232 protocol with eight data bits, no parity, one stop bit, and no flow control. A standard packet will contain the information-formatted vis-à-vis the Student Payload Serial Connection section of the HASP-Student Interface Document.

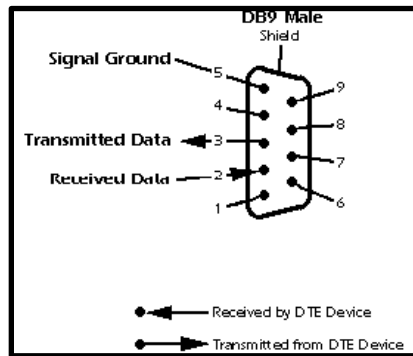


Fig. 13 DB9 pin diagram (Courtesy: HASP manual)

Downlink Telemetry Specifications

(a) Serial data downlink format:

Packetized- Record +/- 232 bytes transmitting in 5 second intervals

(b) Approximate serial downlink rate: 372 bps

- (c) Table-6 shows the information about serial data record including record length and information contained in each record byte. Total record length: 238 bytes

Table-6 Data record length

Byte #	Description	Example	Units
1 - 4	Packet Sync	HASP	n/a
5 - 8	GPS Source	XGPS	n/a
9 - 23	Time stamp	,1407604205.265	sec
24 - 29	Altitude	,38044	m
30 - 35	Sensor 1-1	,01067	ohms
36 - 41	Sensor 1-2	,01390	ohms
42 - 47	Sensor 1-3	,01438	ohms
48 - 53	Sensor 1-4	,01248	ohms
54 - 59	Sensor 1-5	,01282	ohms
60 - 65	Sensor 1-6	,01450	ohms
66 - 71	Sensor 1-7	,01358	ohms
72 - 77	Sensor 1-8	,01060	ohms
78 - 83	Sensor 2-1	,01623	ohms
84 - 89	Sensor 2-2	,02874	ohms
90 - 95	Sensor 2-3	,02999	ohms
96 - 101	Sensor 2-4	,01820	ohms
102 - 107	Sensor 2-5	,01993	ohms
108 - 113	Sensor 2-6	,02956	ohms
114 - 119	Sensor 2-7	,02812	ohms
120 - 125	Sensor 2-8	,01371	ohms
126 - 131	Sensor 3-1	,01495	ohms
132 - 137	Sensor 3-2	,01652	ohms
138 - 143	Sensor 3-3	,01669	ohms
144 - 149	Sensor 3-4	,01748	ohms
150 - 155	Sensor 3-5	,01720	ohms
156 - 161	Sensor 3-6	,01619	ohms
162 - 167	Sensor 3-7	,01506	ohms
168 - 173	Sensor 3-8	,01441	ohms
174 - 179	Temp 1	,00298	K
180 - 185	Temp 2	,00309	K
186 - 191	Temp 3	,00297	K
192 - 197	Photovoltage 1	,00460	mV
198 - 203	Photovoltage 2	,00464	mV
204 - 209	Photovoltage 3	,00467	mV
210 - 215	CPU Temp	,00304	K
216 - 221	Power Rail Voltage	,03317	mV
222 - 227	Power Rail Current	,00148	mA
228 - 233	Pressure	,00117	mBar
234 - 238	Heater Status	,1101	n/a

The standard RS-232 connectivity rate for a small payload is 1200 baud. We will certainly try to remain within the limit this time by improving our software program and hardware.

- (d) Number of analog channels being used: 0
 (e) Number of discrete lines being used: 0
 (f) Are there any on-board transmitters? No.
 (g) Other relevant downlink telemetry information. Not Applicable

3.4 Uplink Serial Commanding

Command uplink capability required: Yes

- (h) If so, will commands be uplinked in regular intervals: No
 (i) How many commands do you expect to uplink during the flight (can be an absolute number or a rate, i.e., *n commands per hour*): 1 command per hour maximum
 (j) Provide a table of all the commands that you will be up linking to your payload

The proposed commands are mentioned in the table-7 (a) and (b). Any changes in the list will be updated at the time of PSIP and FLOP.

Table 7 (a): List of Commands in general

#	Command Description	Cmd. Code	Checksum	Confirmation/Notes
1	Reset	0x71	0x31	"HELLO" upon reset
2	Erase data in flash	0x72	0x32	"ERASING FLASH"..." COMPLETE"

3	Upload data in flash	0x73	0x33	"NO DATA"
4	n/a	n/a	n/a	n/a
5	Master Heater Override Switch On	0x75	0x35	Heater Status (default)
6	Master Heater Override Switch Off	0x76	0x36	Heater Status
7	On Board Data Logging On	0x77	0x37	Data (default)
8	On Board Data Logging Paused	0x78	0x38	Data empty
9	Stream UNF GPS data	0x79	0x39	"UGPS"
10	Stream HASP GPS data	0x7A	0x3A	"HGPS"

Table 7 (b) List of Uplink Commands

Command	Hex Code	Description	Importance
RESET	7131	Reset System	Critical
HEATER OVERRIDE_ON	7535	Turn Master Heater Switch Off. The main heater switch is disabled so no individual heaters will be able to turn ON.	Critical
HEATER OVERRIDE_OFF	7636	Turn Master Heater Switch On (default). The main heater switch is enabled and thus each individual heater can turn ON or OFF as needed by the temperature controller.	Critical
UBLOX_STREAM	7939	Stream GPS via Embedded GPS (default)	Critical
HASP_STREAM	7A3A	Stream GPS via HASP GPS	Critical

(k) Other relevant uplink commanding information. None

3.5 Analog Downlink

None

3.6 Discrete Commanding

None

3.7 Payload Location and Orientation Request

The requested smaller payload should be oriented on the side away from any solar cells to avoid disparate solar thermal radiation. There should not be any obstacle for air circulation into payload and any shadow of other payload. We would like the position of the payload (#7) on HASP to be the same as in the previous flights. Fig. 14 (a) and (b) shows our desired location of payload on HASP.

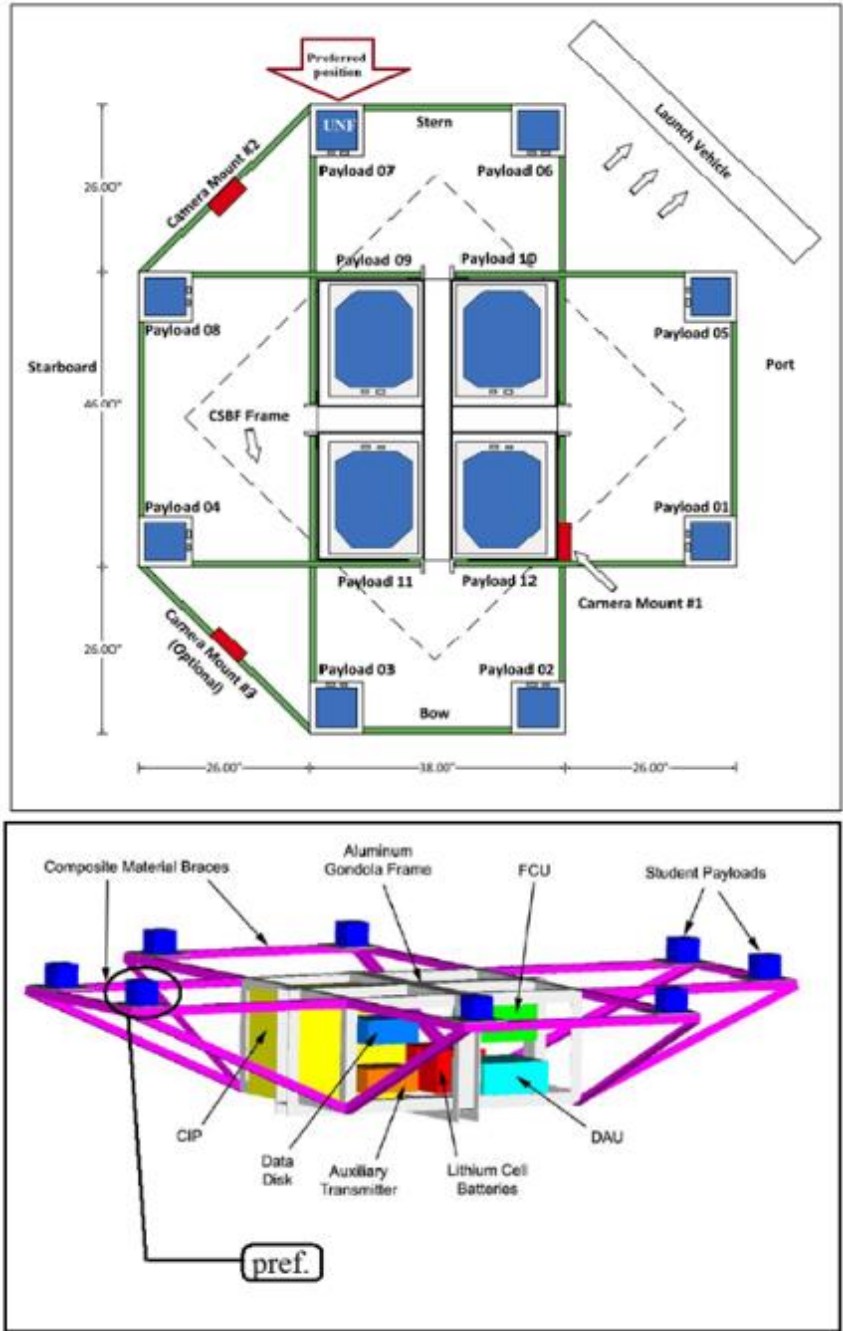


Fig. 14 (a) Top view (b) side view proposed HASP Configuration
 Dr. Guzik and Wefel [11]

http://laspace.lsu.edu/hasp/documents/public/HASP_Interface_Manual_v21709.pdf

3.8 Special Request

We request the HASP to provide us the GPS strings from the HASP gondola every 1 second in case of failure of our payload GPS.

4 Preliminary Drawings and Diagrams

Kindly refer Appendix-A Page # 41 to 55 for mechanical drawings and Appendix-B Page # 56 to 65 for electrical drawings. Any changes in drawing will be update in the PSIP and FLOP documents.

5. References

- [1] Perry J. Samson, “Nocturnal Ozone Maxima”
Atmospheric Environment, Vol.12 (1978) 951-955.
 - [2] A. Mavrakis, H. Flocas, E. Mavromatidis, G. Kallos, G. Theoharatos and A. Christides, “A Case of Nighttime High Ozone Concentration over the Greater Athens Area”, Meteorologische Zeitschrift, Vol. 19, No.1 (2010) 035-045.
 - [3] R. San Jose, A. Stohl, K. Karatzas, T. Bohler, P.James and J.L. Perez, “A Modelling Study of an Extraordinary Nighttime Ozone Episode over Madrid Domain”. Environmental Modelling & Software 20 (2005) 587-593.
 - [4] Solid-State Sensors Behavior in Reduced Pressure Environments Demonstration Using an Experimental Indium Tin Oxide Ozone Gas Sensors for Ozone Sounding; Nathan Ambler, Ronald Fevig and Nirmal Patel, Proceedings of 59th International Astronautical Congress, Glasgow, (Sept 29-Oct 3, 2008), C2. I.17
 - [5] Hansford, Graeme M., et al. "A low cost instrument based on a solid state sensor for balloon-borne atmospheric O₃ profile sounding." Journal Environmental Monitoring (2005): 158-162.
 - [6] Nanocrystalline Indium Tin Oxide Sensors and Associated method of use.
U.S. Patent No.:10,823,690 B2 Nov. 3. 2020.
 - [7] Nanocrystalline indium tin oxide sensors and arrays.
U.S Patent No. 9,606,078 B2, March 28, 2017.
 - [8] Quartz crystal microbalance with nanocrystalline oxide semiconductor thin films and method of detecting vapors and odors including alcoholic beverages, explosive materials and volatilized chemical compounds.
U.S Patent No. 7,930,923 B2, April 26, 2011
 - [9] HASP – Student Payload Interface Manual, Version 02.17.9
http://laspace.lsu.edu/hasp/documents/public/HASP_Interface_Manual_v21709.pdf
 - [11] Guzik, T. Gregory and John P. Wefel. "The High Altitude Student Platform (HASP) for Student-Built Payloads." 35th COSPAR Scientific Assembly. Houston, Texas, 2004. 1-8.
 - [10] Atkins, Noel. Survey of Meteorology. 10 November 2007
http://apollo.lsc.vsc.edu/classes/met130/notes/chapter1/vert_temp_all.html
-

Appendix- A

Detailed Mechanical Drawings

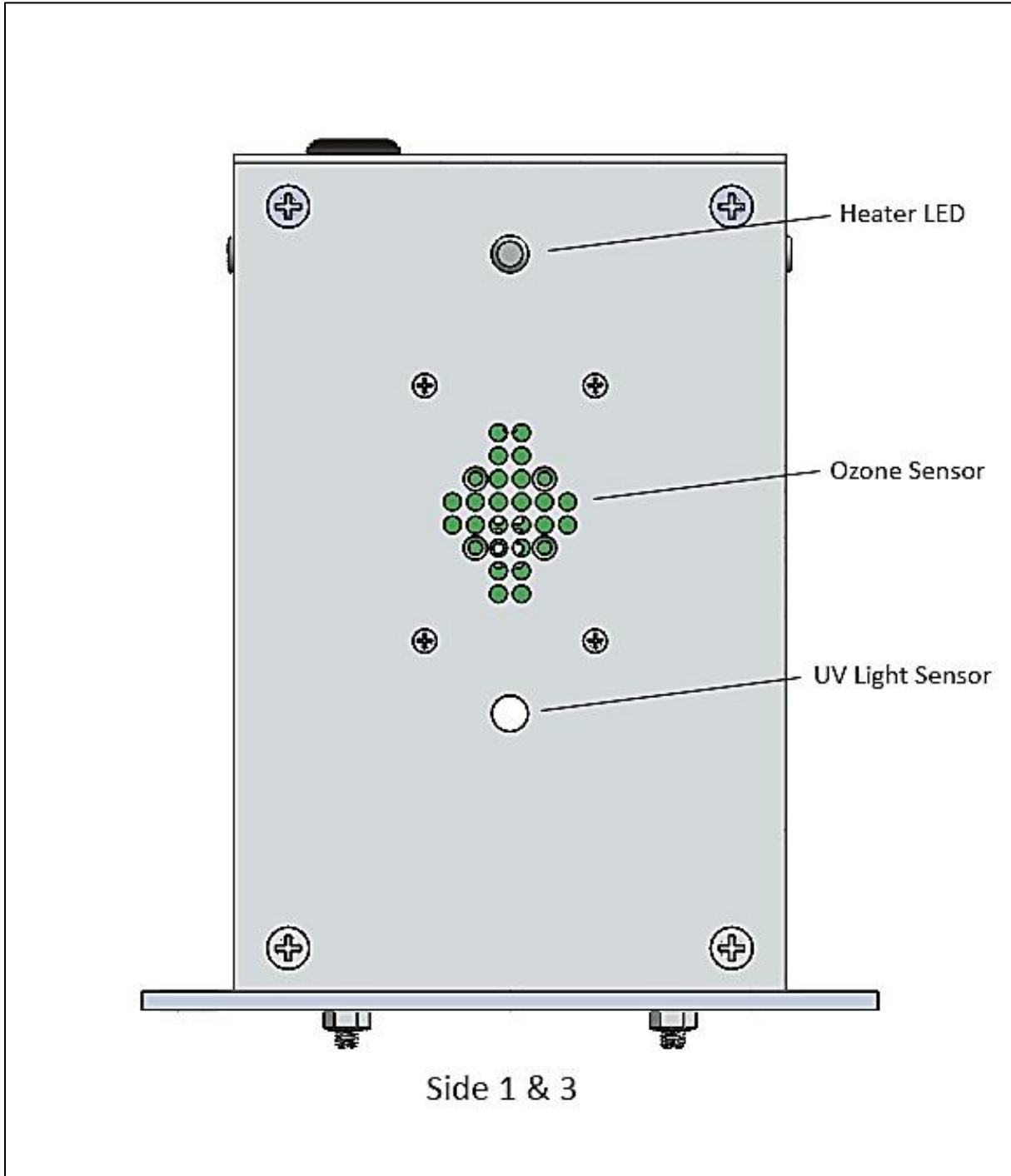


Fig. 4(d) Outer view of design of sides # 1 and 3 of the payload

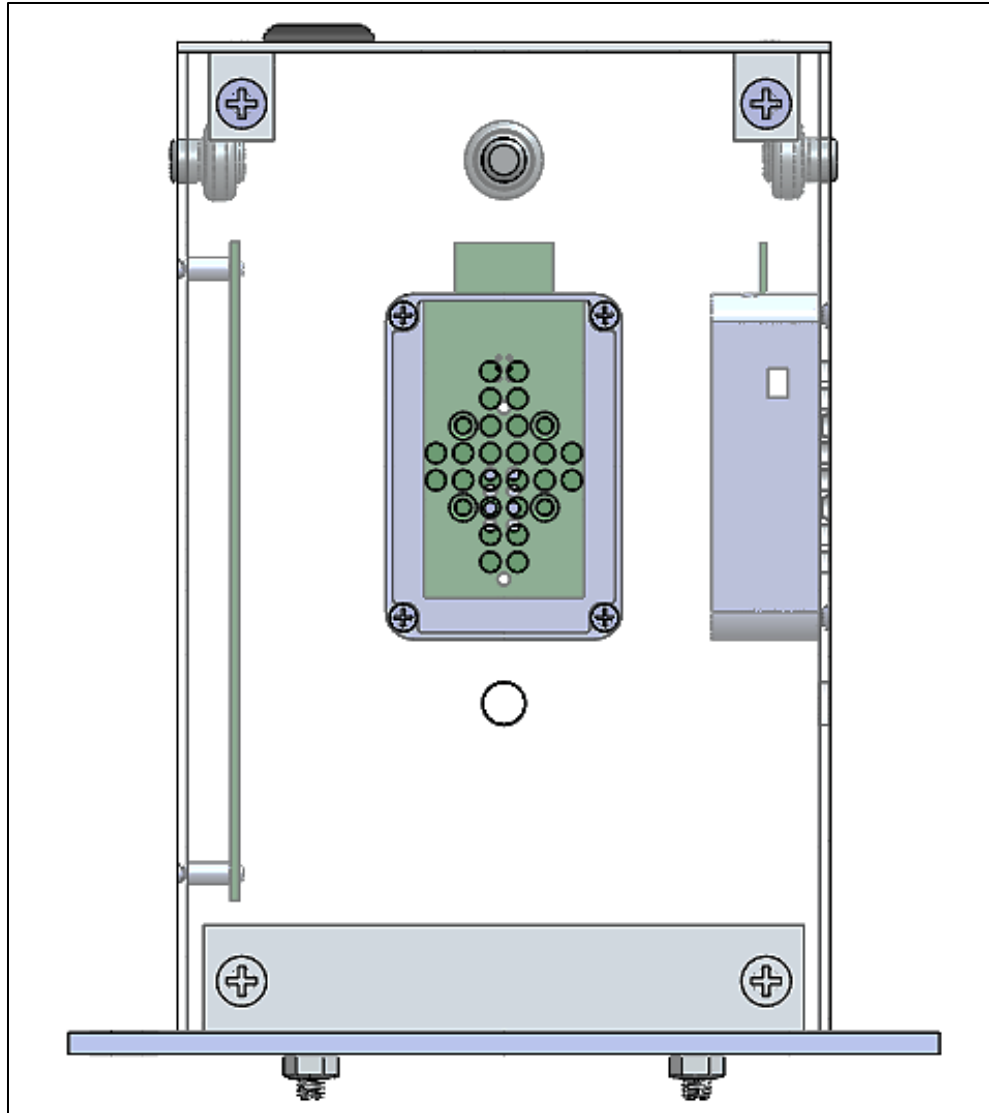


Fig. 4(e) Inside view of design of sides # 1 and 3 of the payload

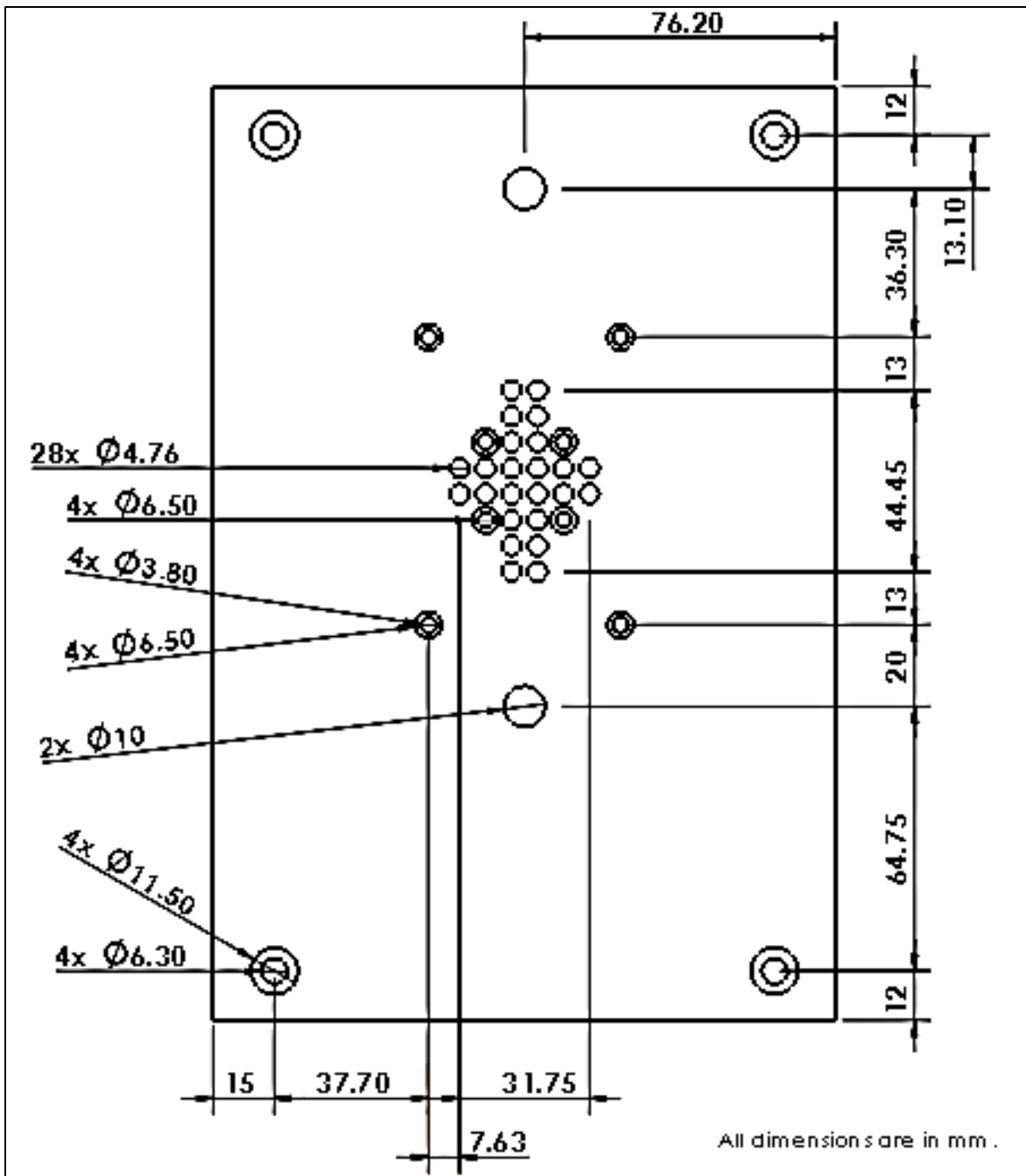


Fig. 4(f) Design with dimensions of sides # 1 and 3 of the payload

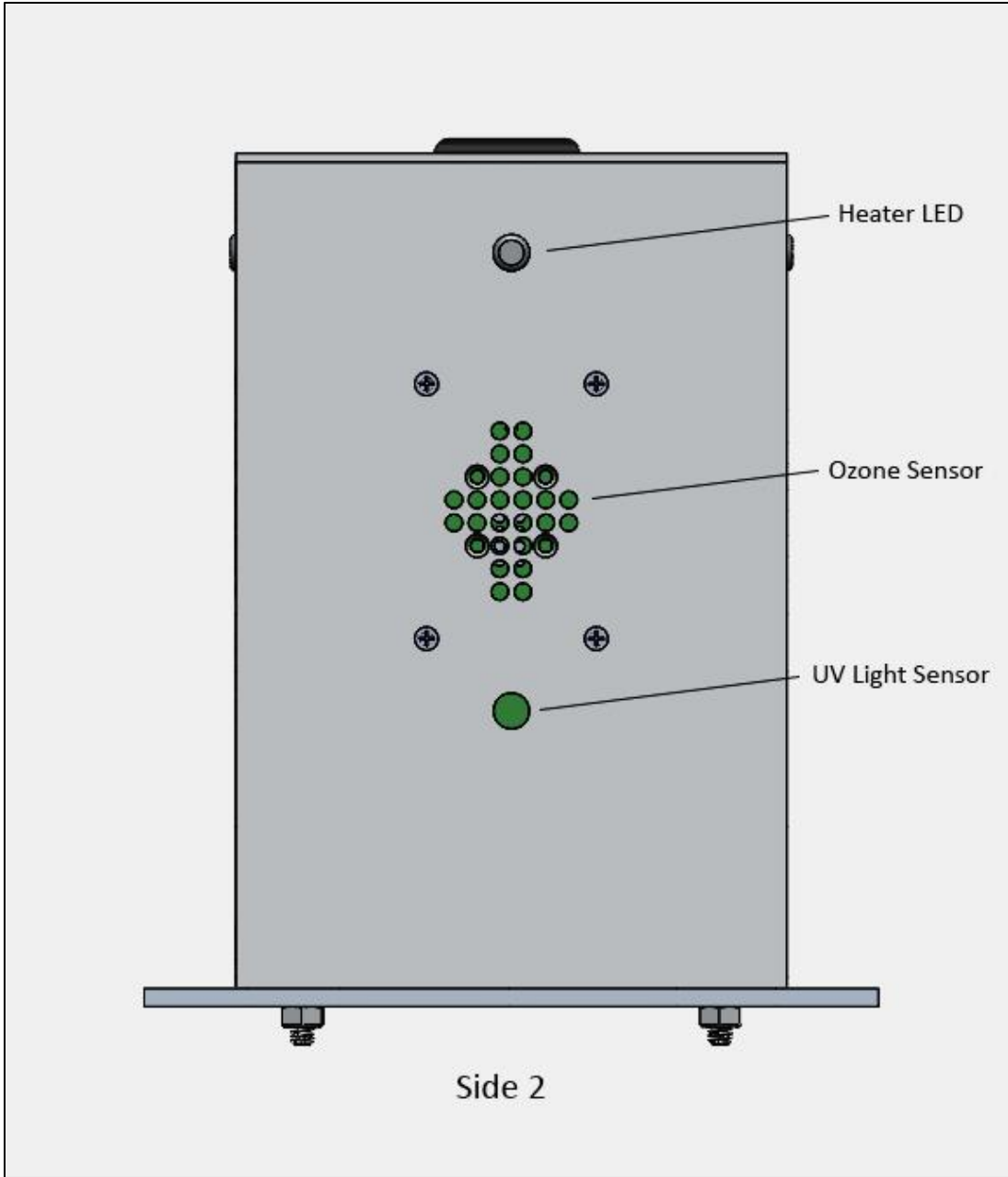


Fig. 4(g) Outer view of design of side # 2 of the payload

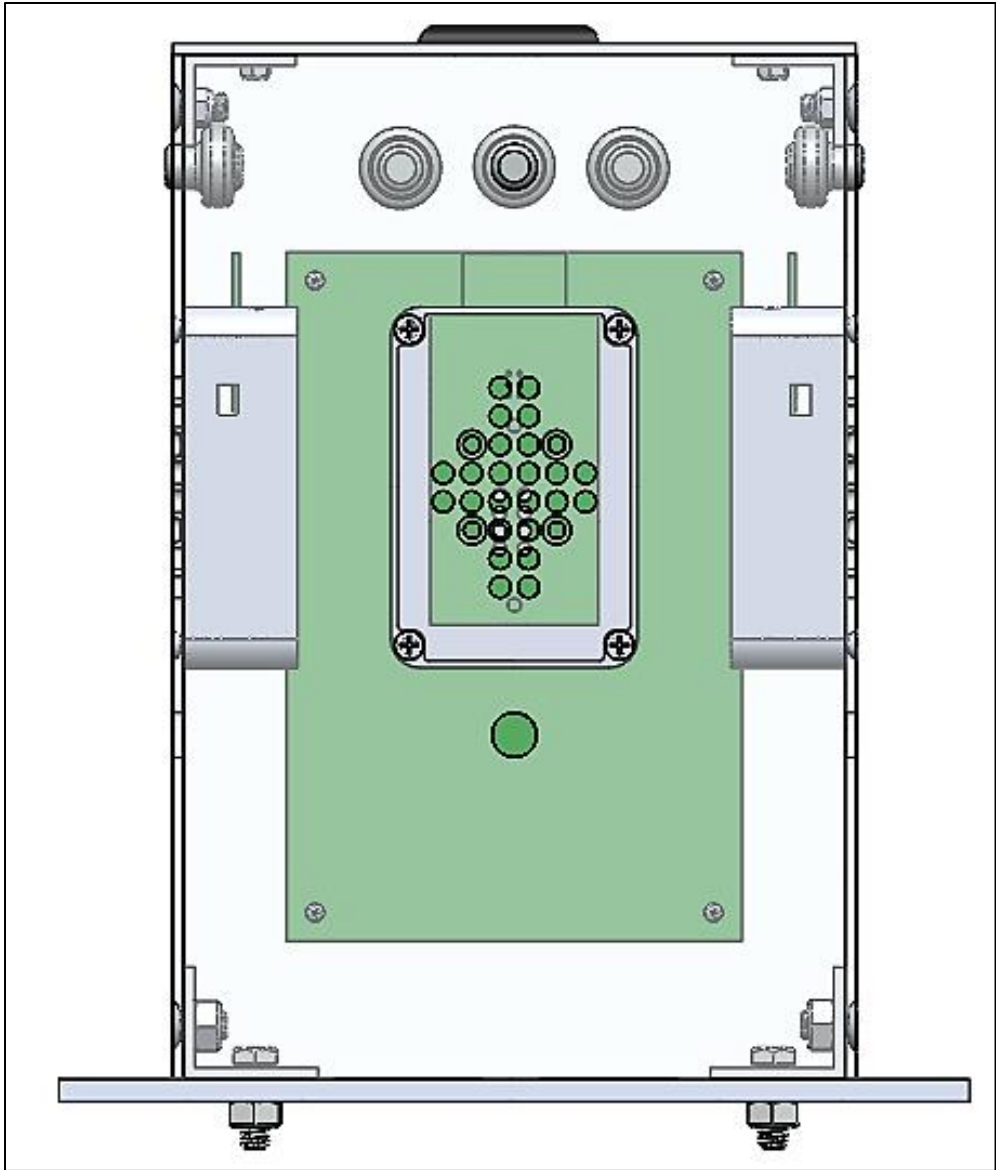


Fig. 4(h) Inside view of design of side # 2 of the payload

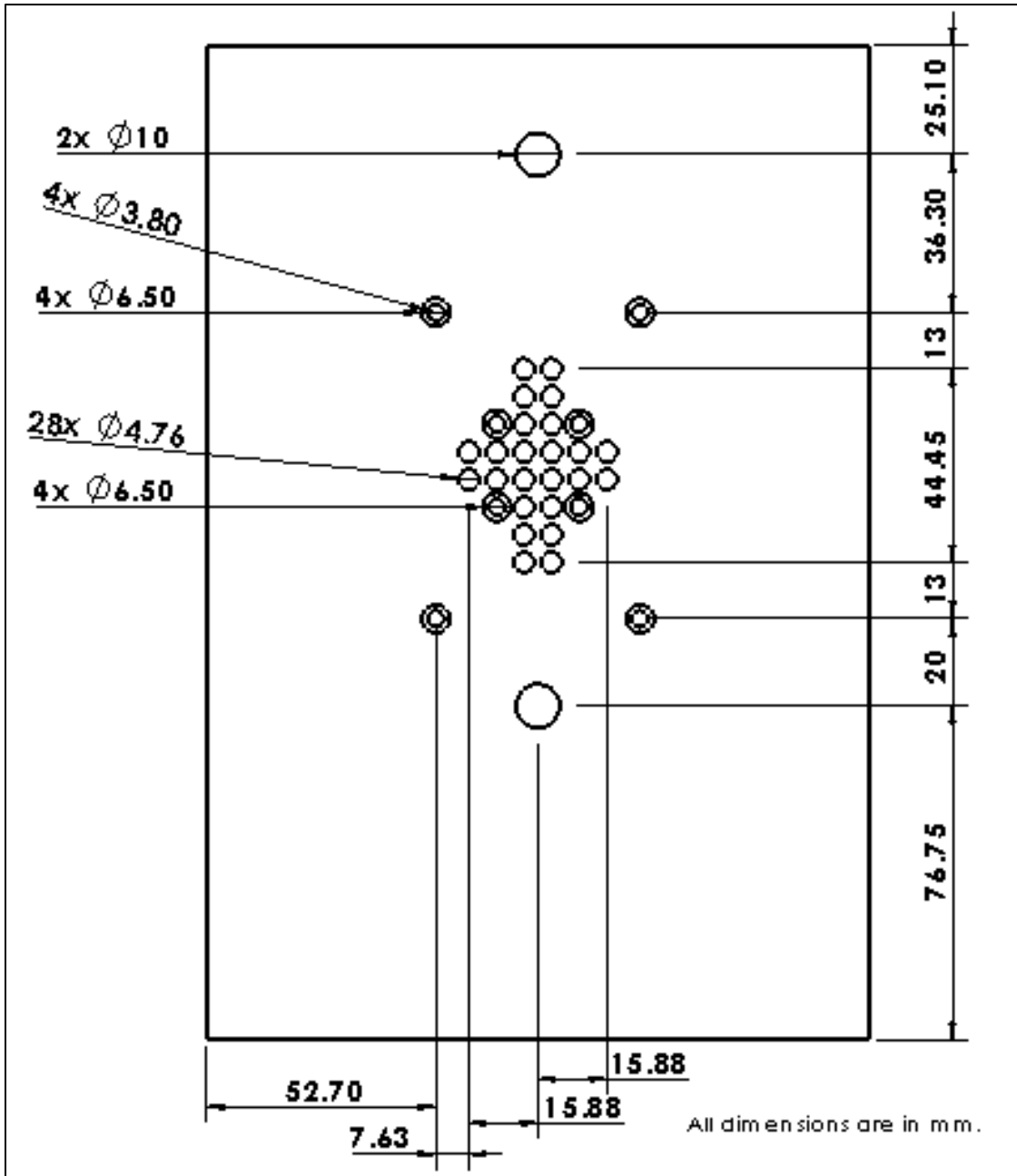


Fig. 4(i) Design with dimensions of side # 2 of the payload

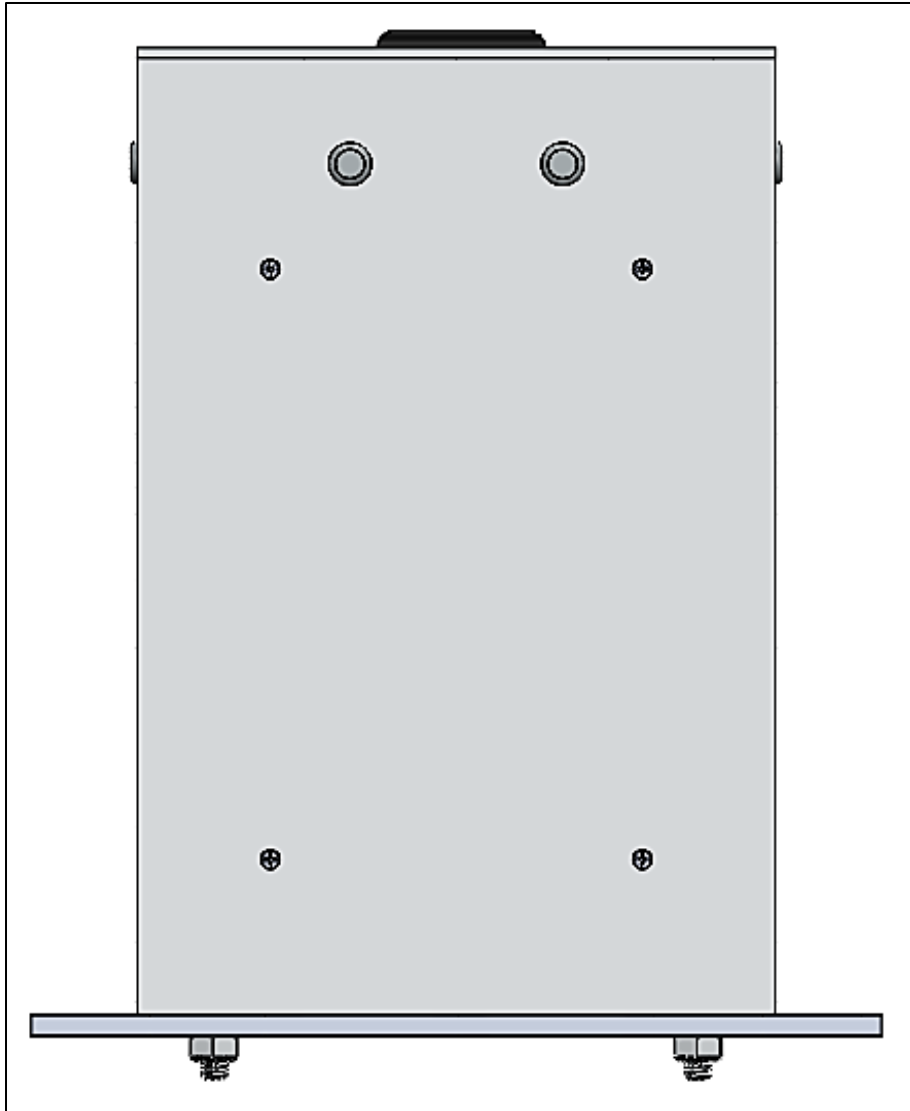


Fig. 4(j) Outer view of design of side # 4 of the payload

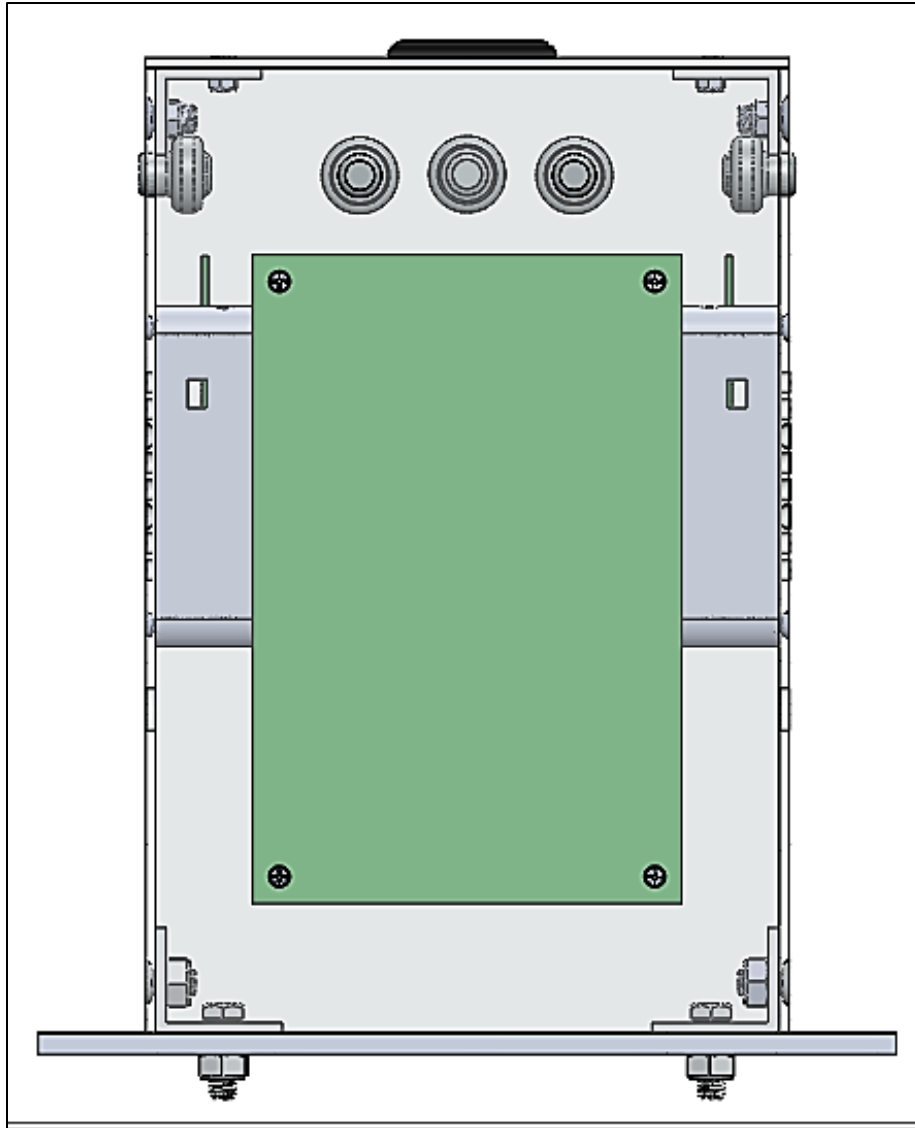


Fig4(k) Inside view of design of side # 4 of the payload.
Microcontroller circuit board (Green color) mounted on side #4

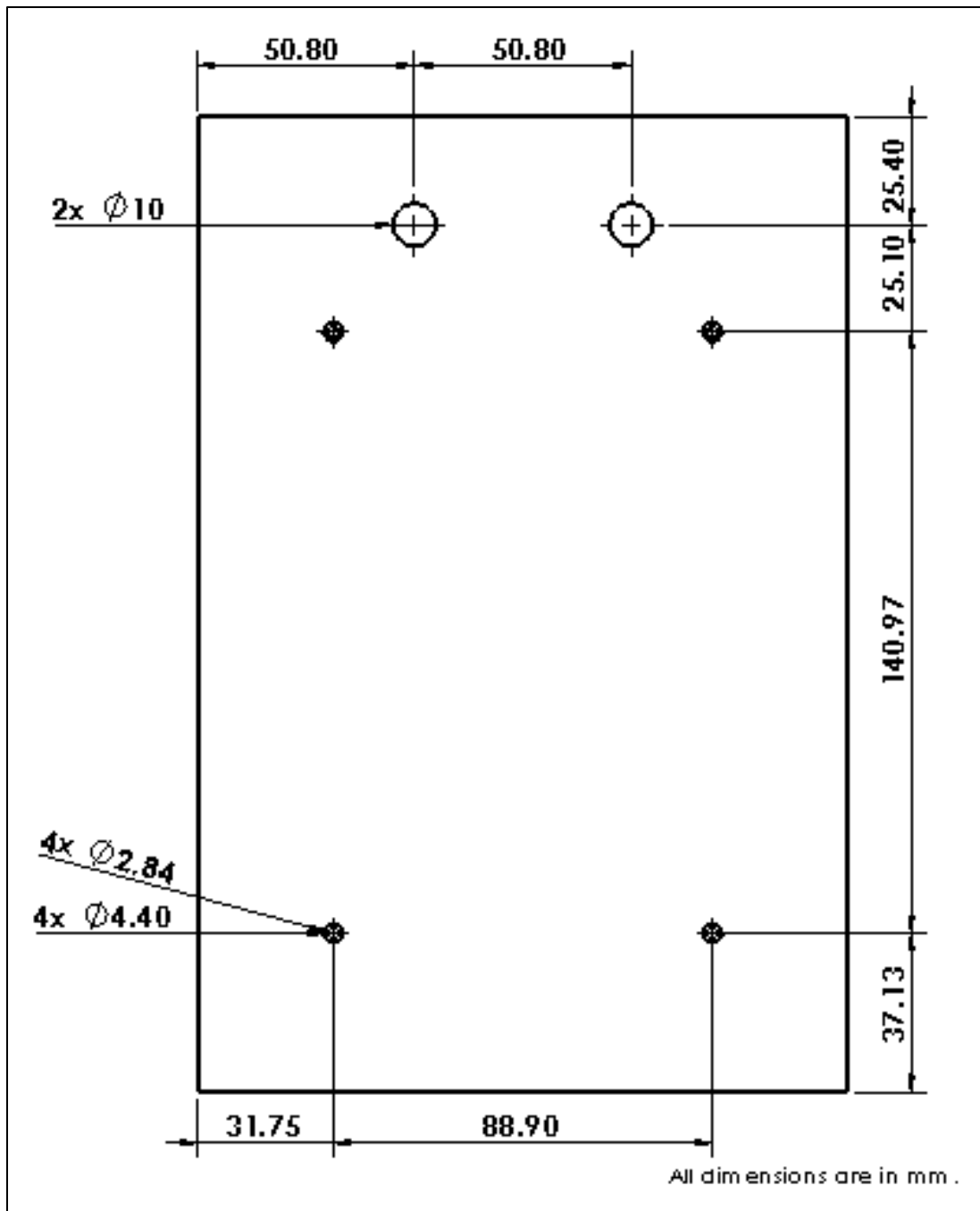


Fig. 4(l) Design with dimensions of side # 4 of the payload

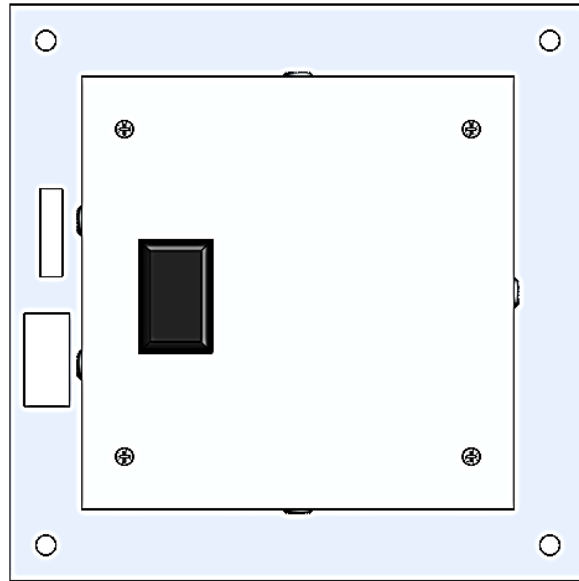


Fig. 4 (m) Design of top plate of the payload

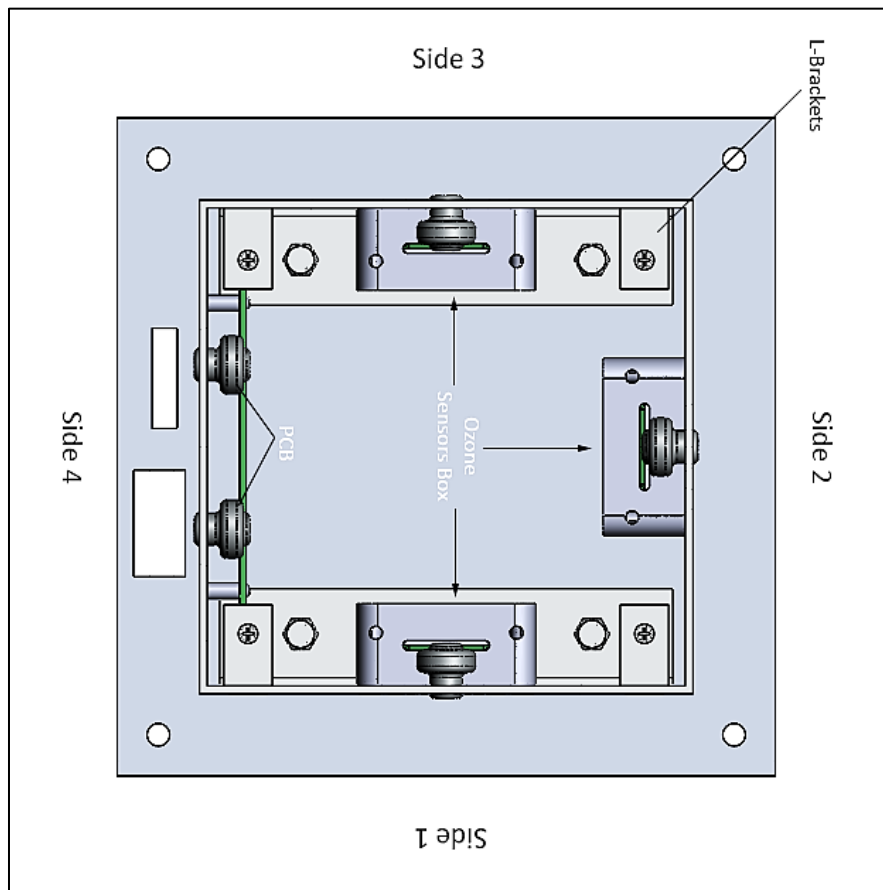


Fig. 4 (n) Top inside view of the payload

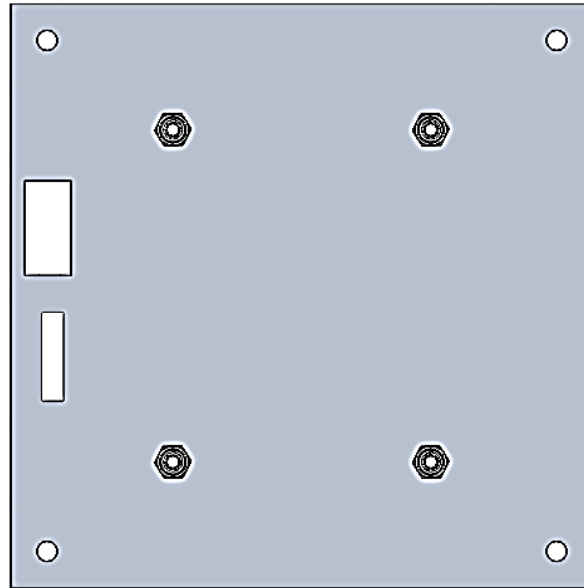


Fig. 4 (o) Bottom outer view of the payload

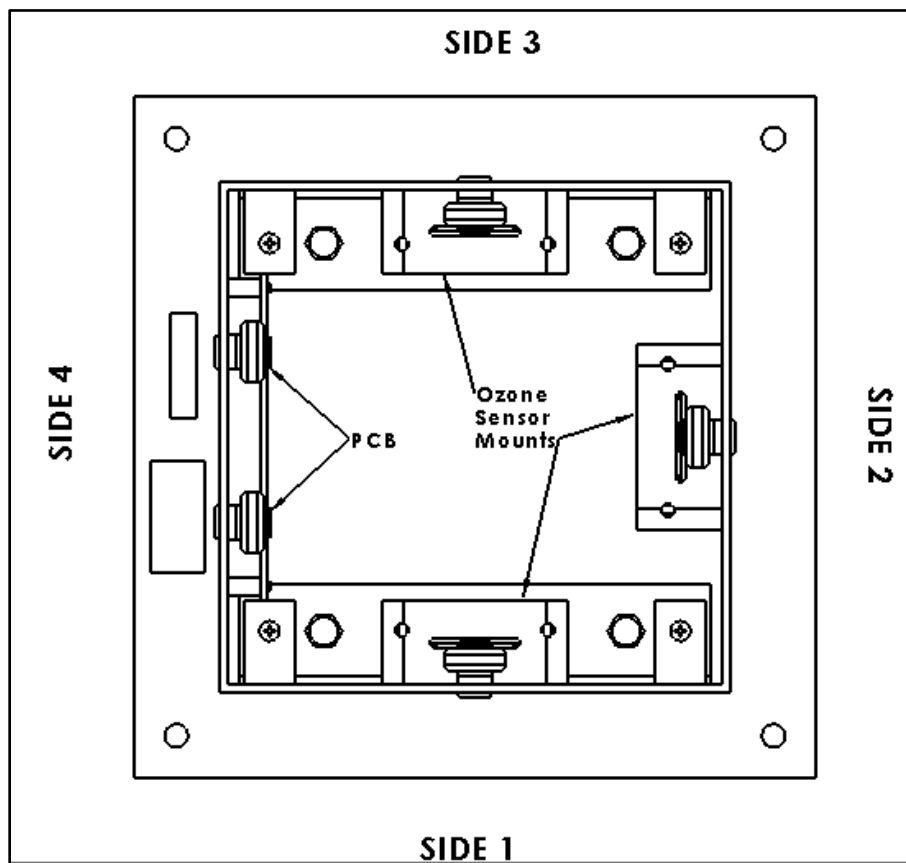


Fig4 (p) Bottom inside view of the payload

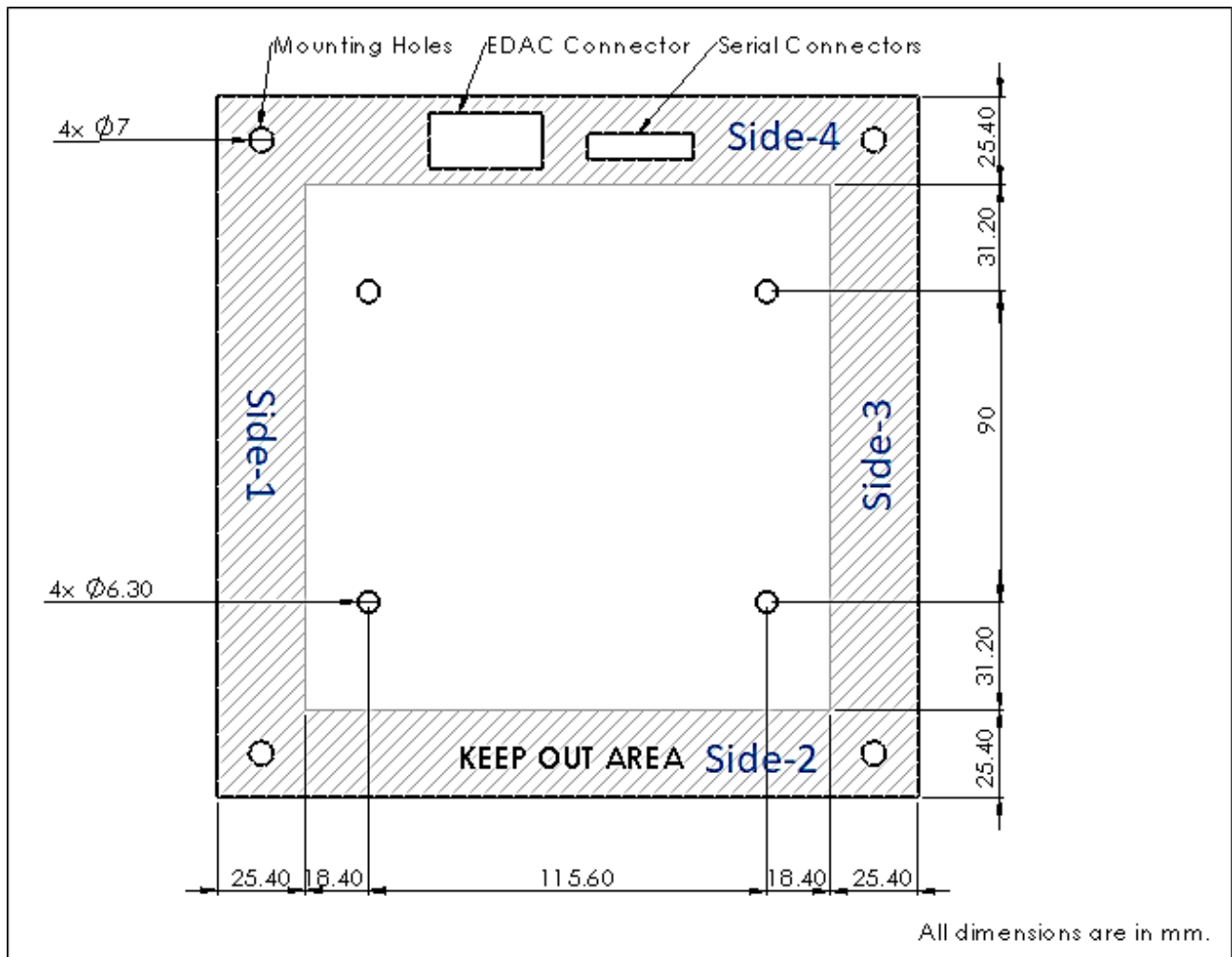


Fig. 4 (q) Design of HASP mounting plate

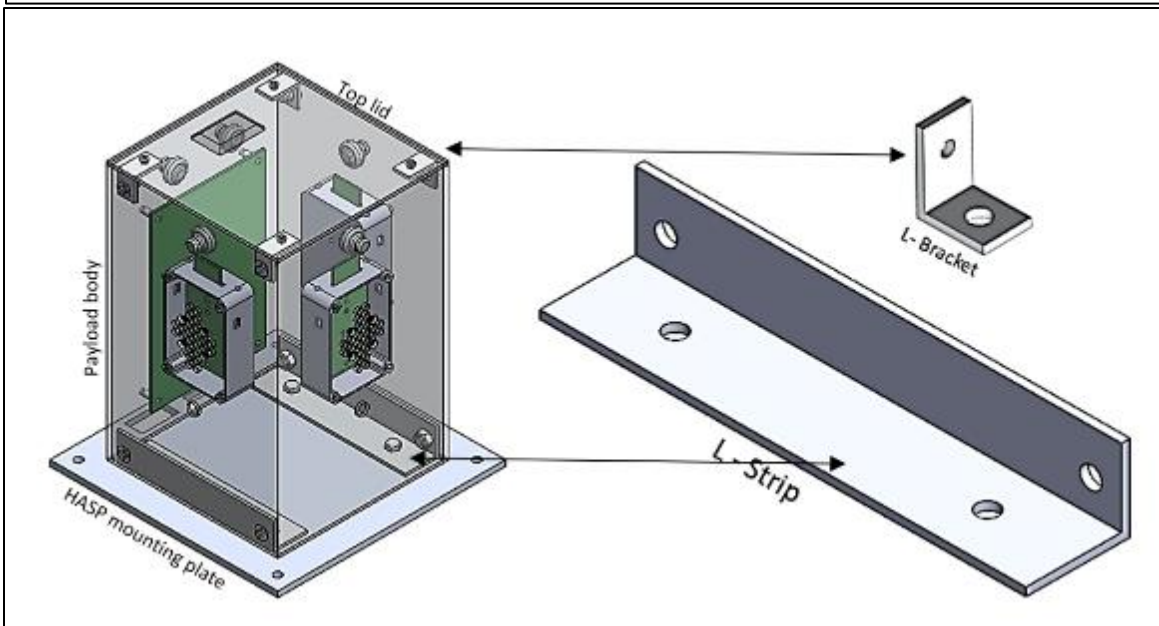
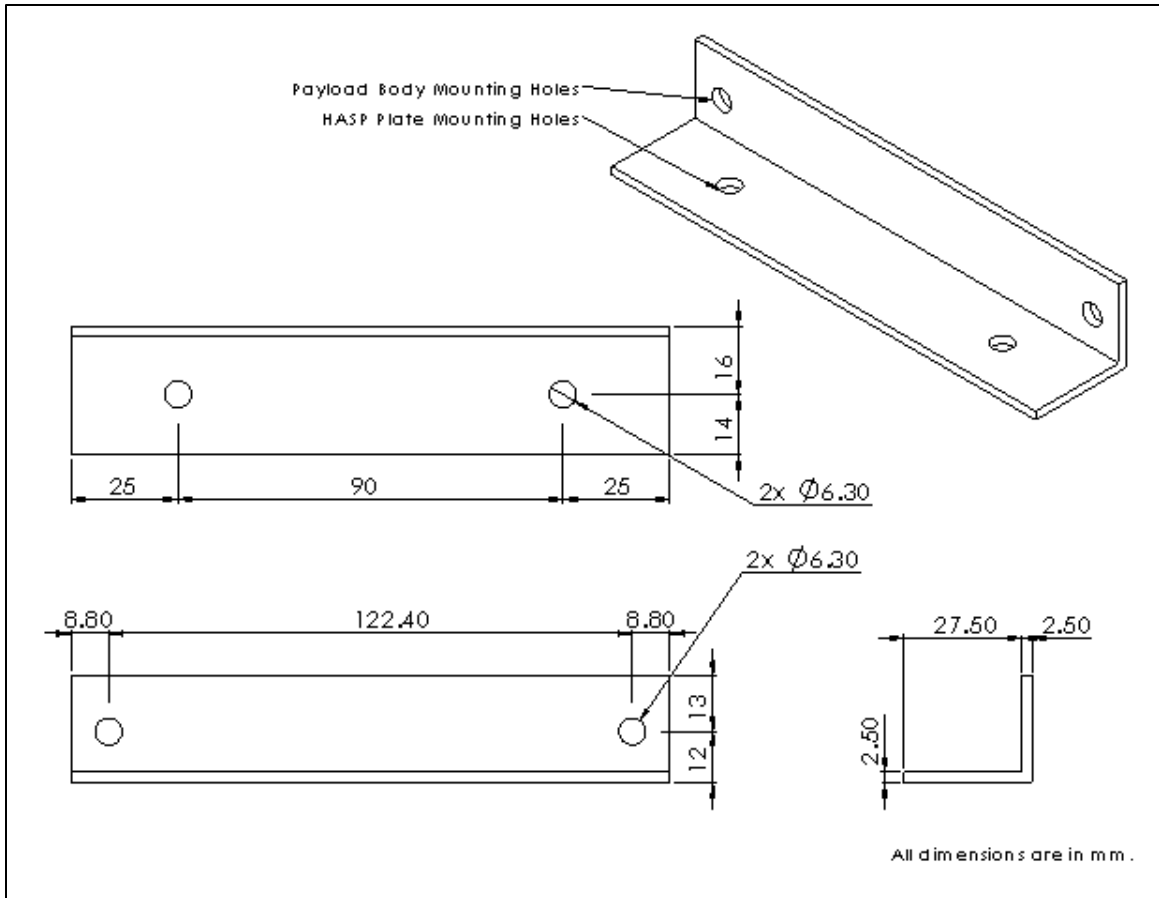


Fig. 4 (s) Design of L-Strip for mounting the HASP plate with payload body and Design of L-Brackets for mounting the top lid on the payload body

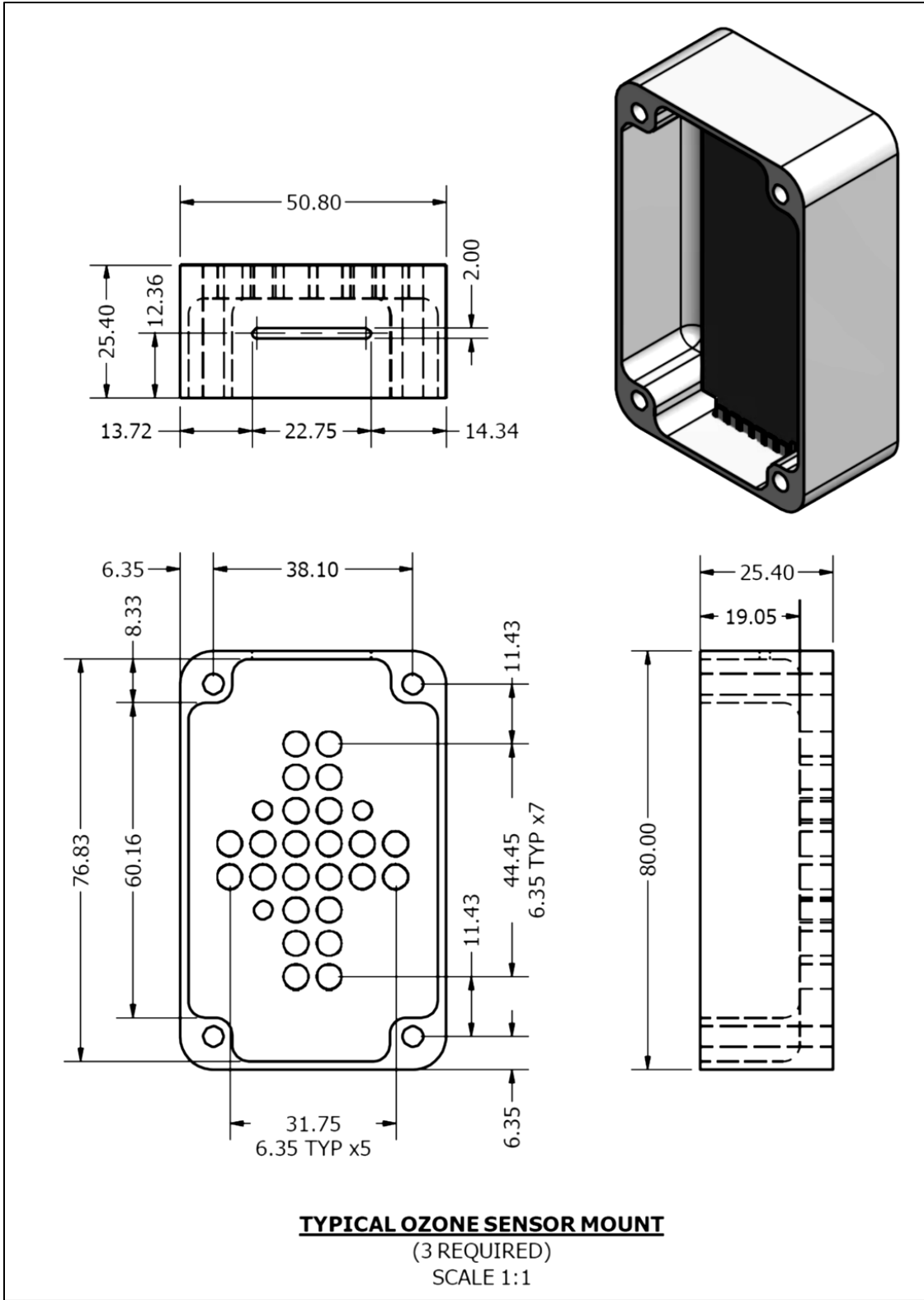


Fig.4 (t) Design of sensor box of the payload
All dimensions are in mm.

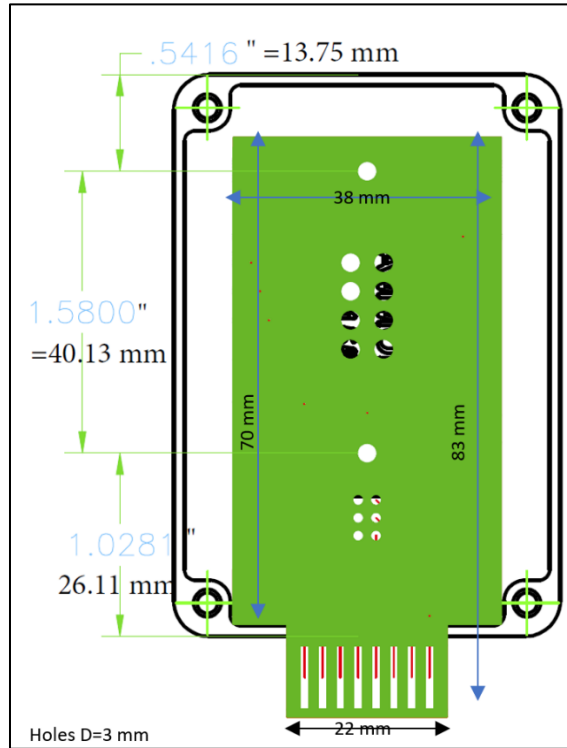


Fig.4 (u) Design for standoff to mount sensor PCB in the box

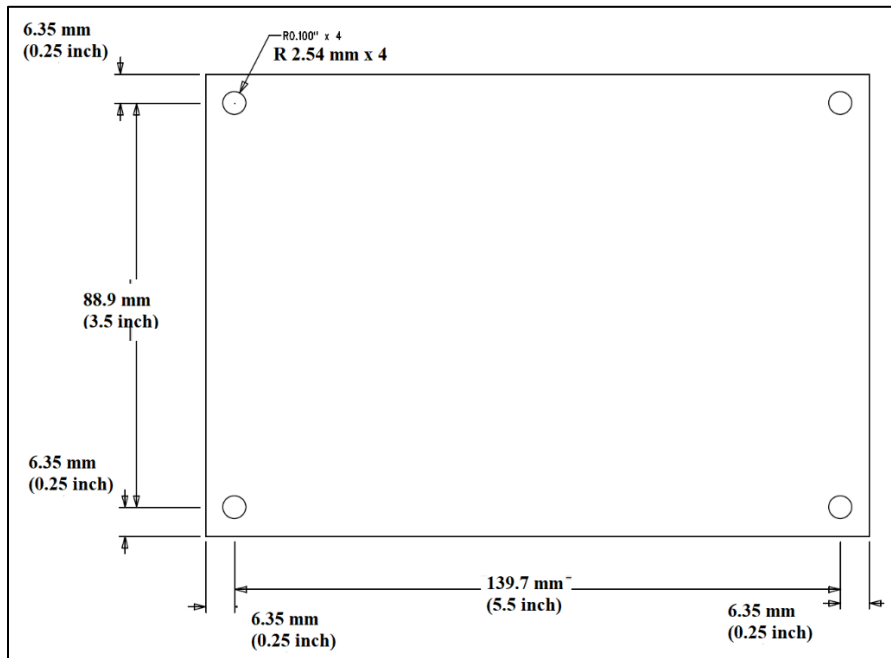


Fig. 4 (v) Design for hole to mount the microcontroller PCB on side # 4.

Appendix -B

Detailed Electronic Circuit Diagrams

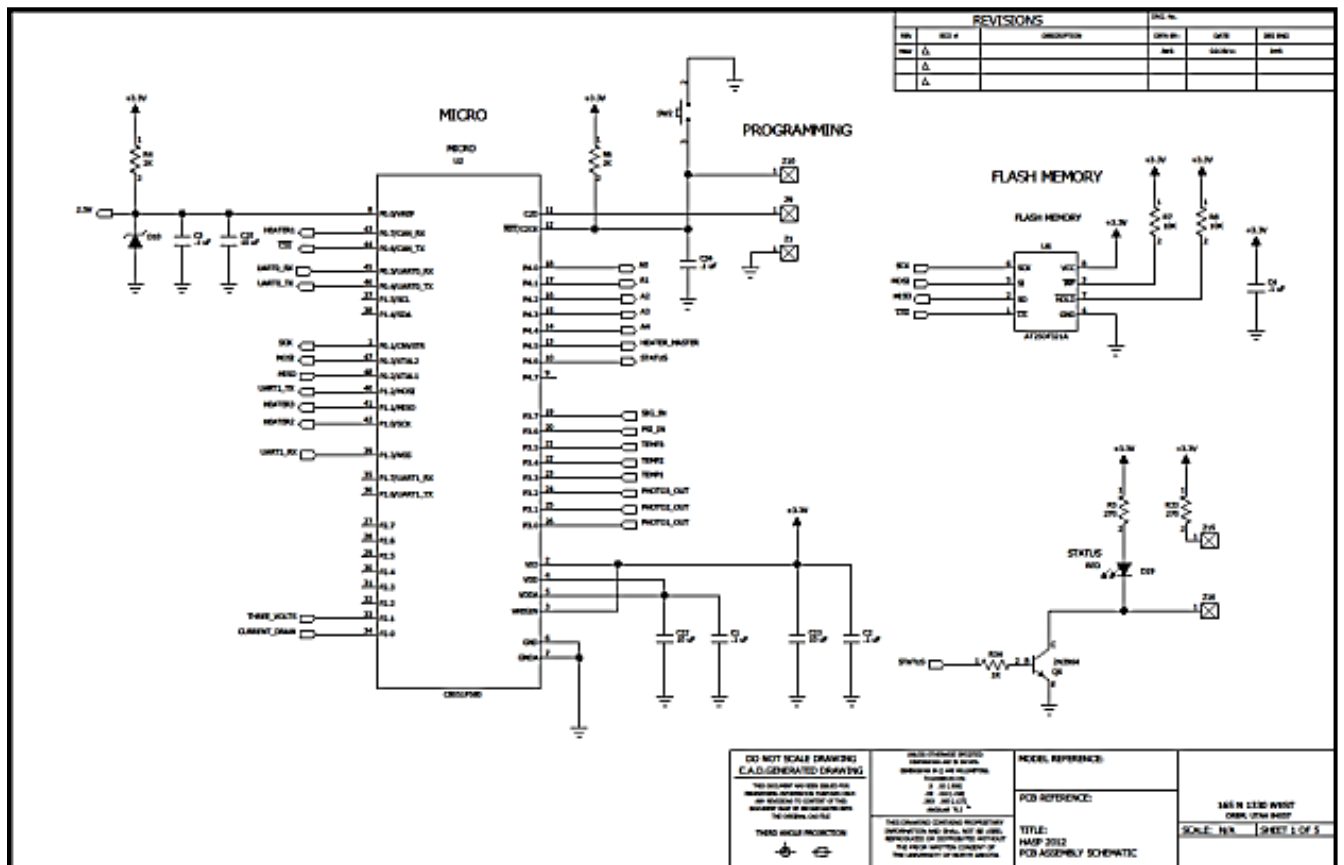


Fig. 6 (b) Circuit for microcontroller and flash memory

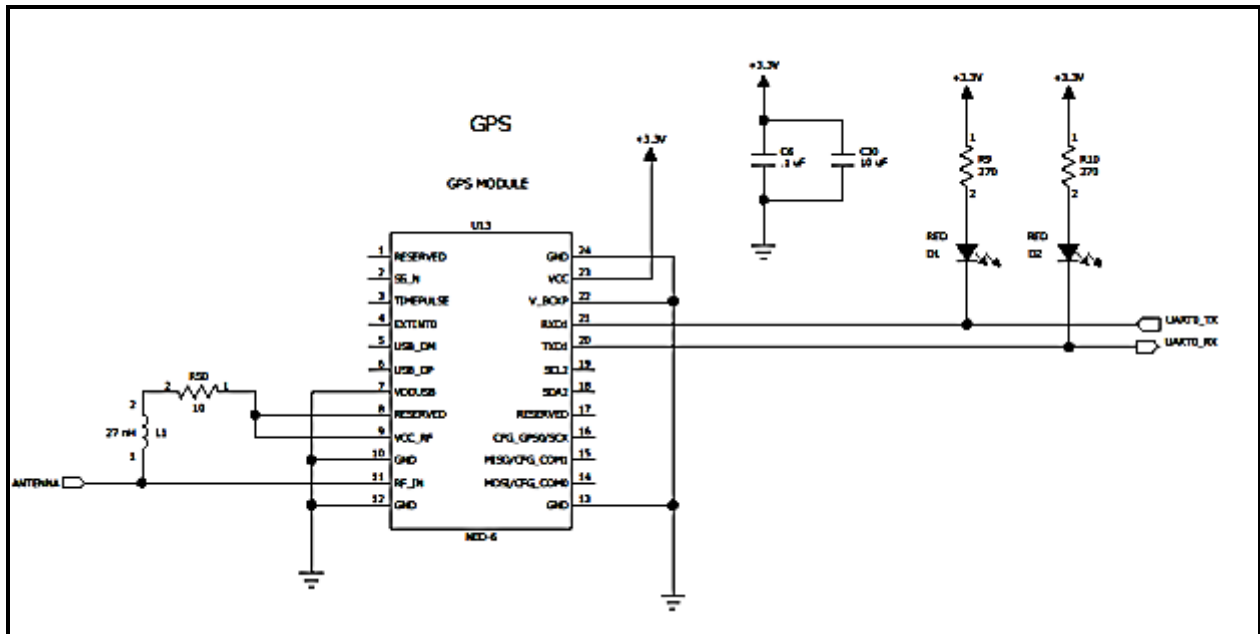


Fig. 6 (c) Circuit for GPS

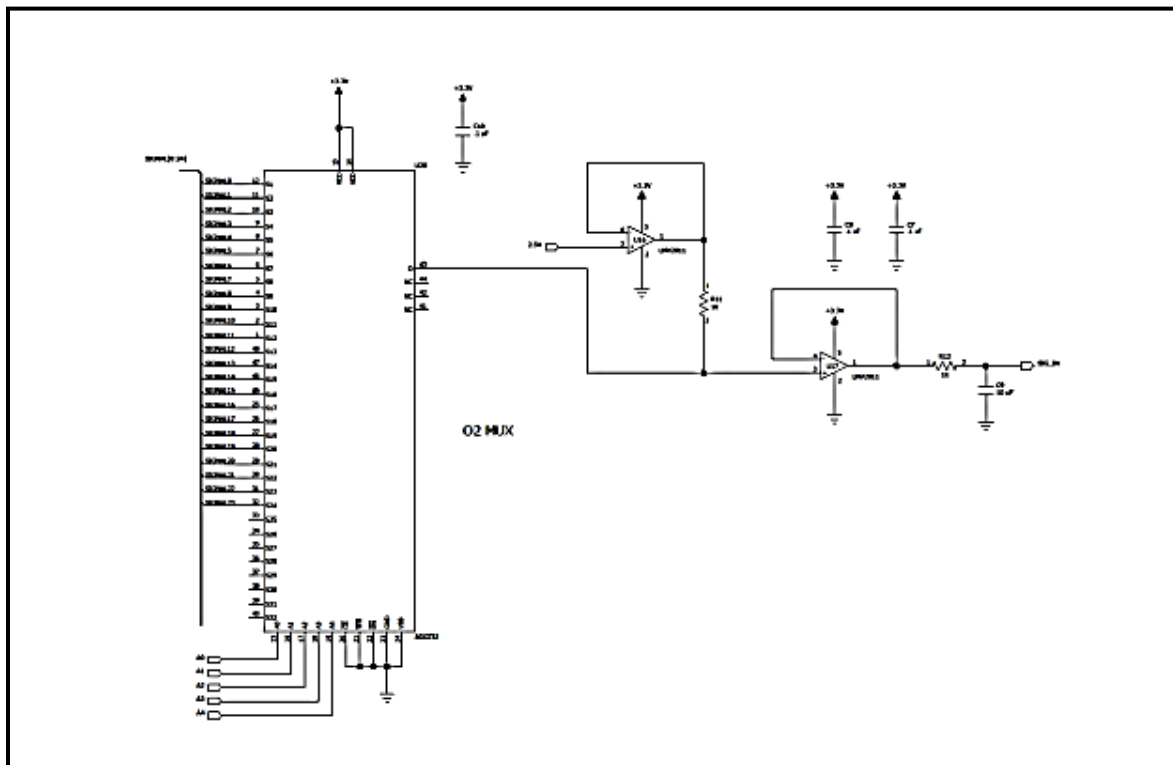


Fig. 6 (d) Multiplexer circuit

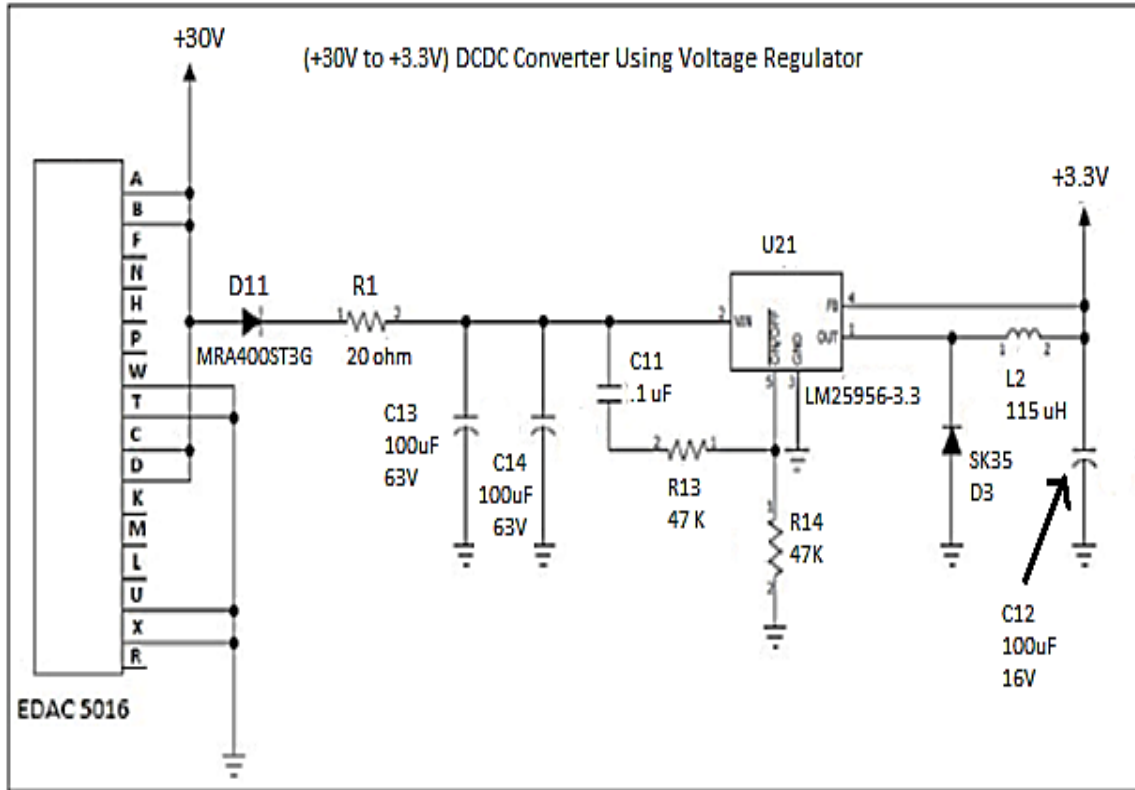


Fig. 6 (e) Voltage regulation circuit

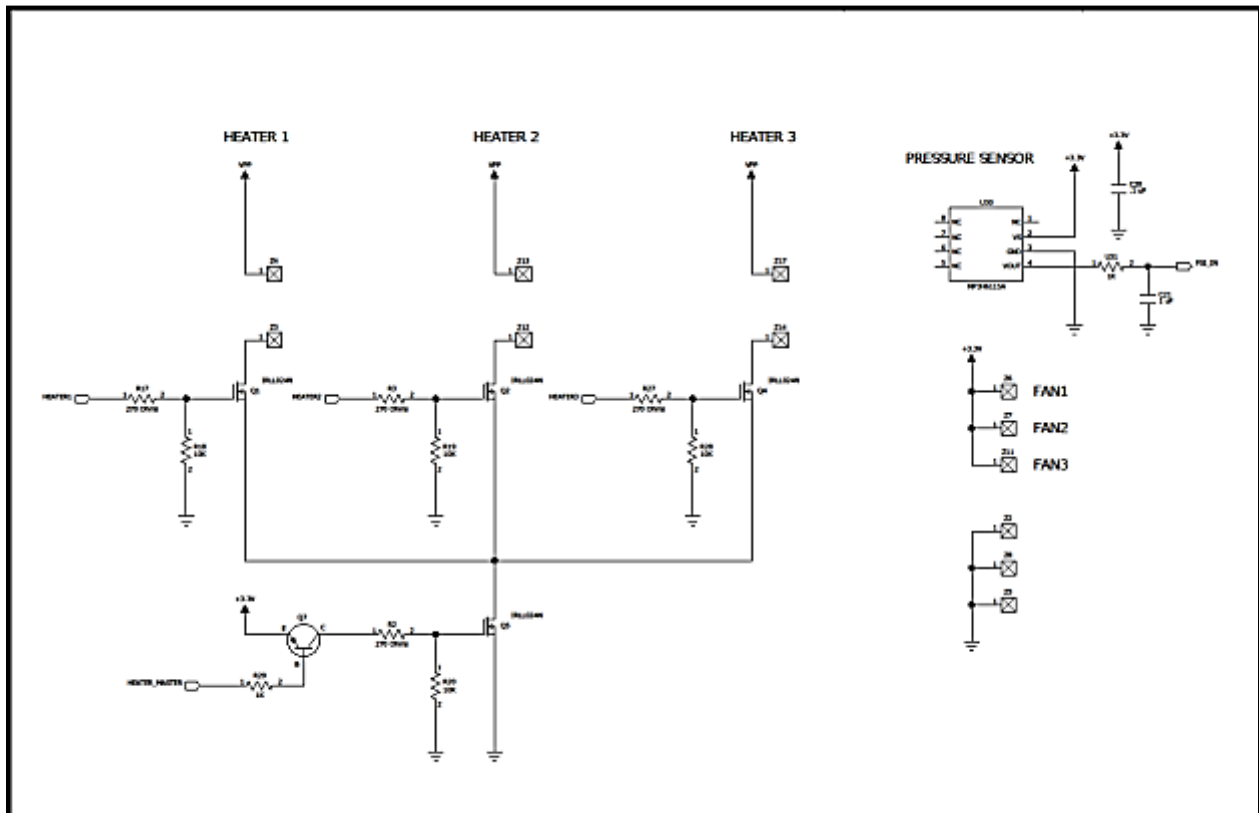


Fig. 6 (f) Circuit for three heaters, three fans and pressure sensor

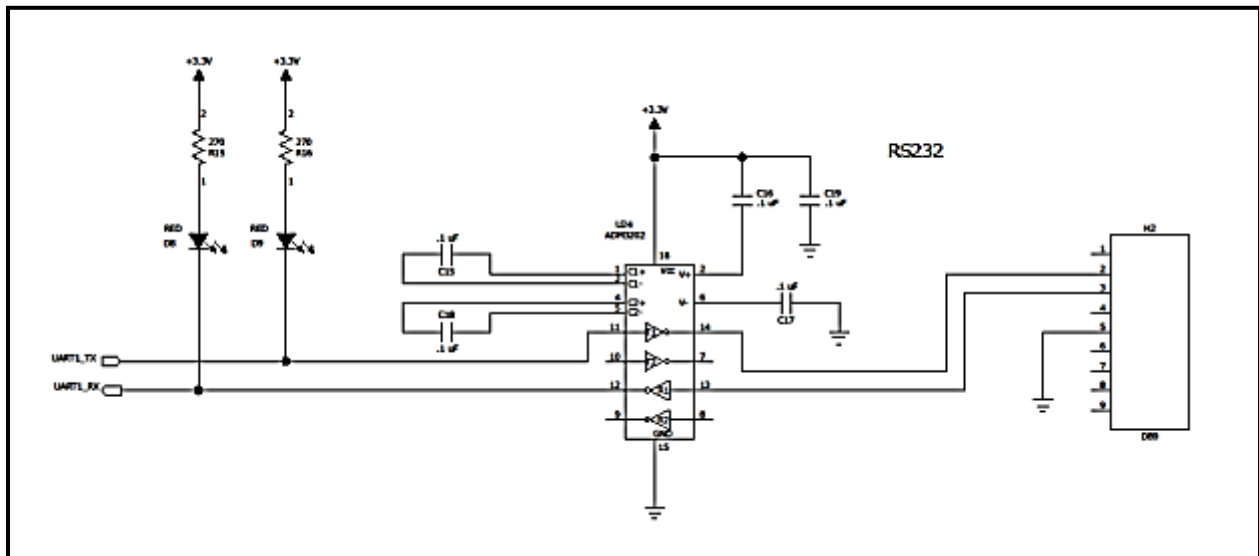


Fig. 6 (g) Circuit for RS232

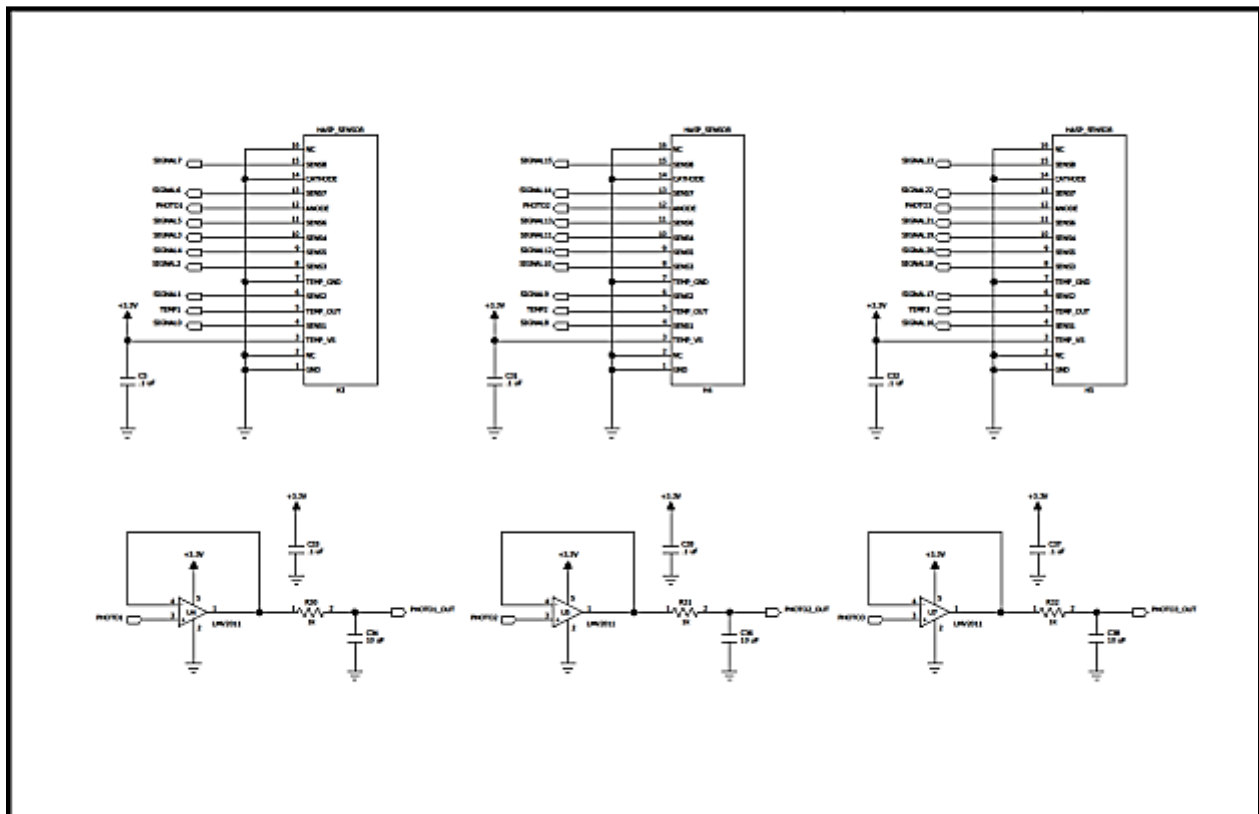


Fig. 6(h) Circuit for three ozone sensors boxes and three photo (light) sensors

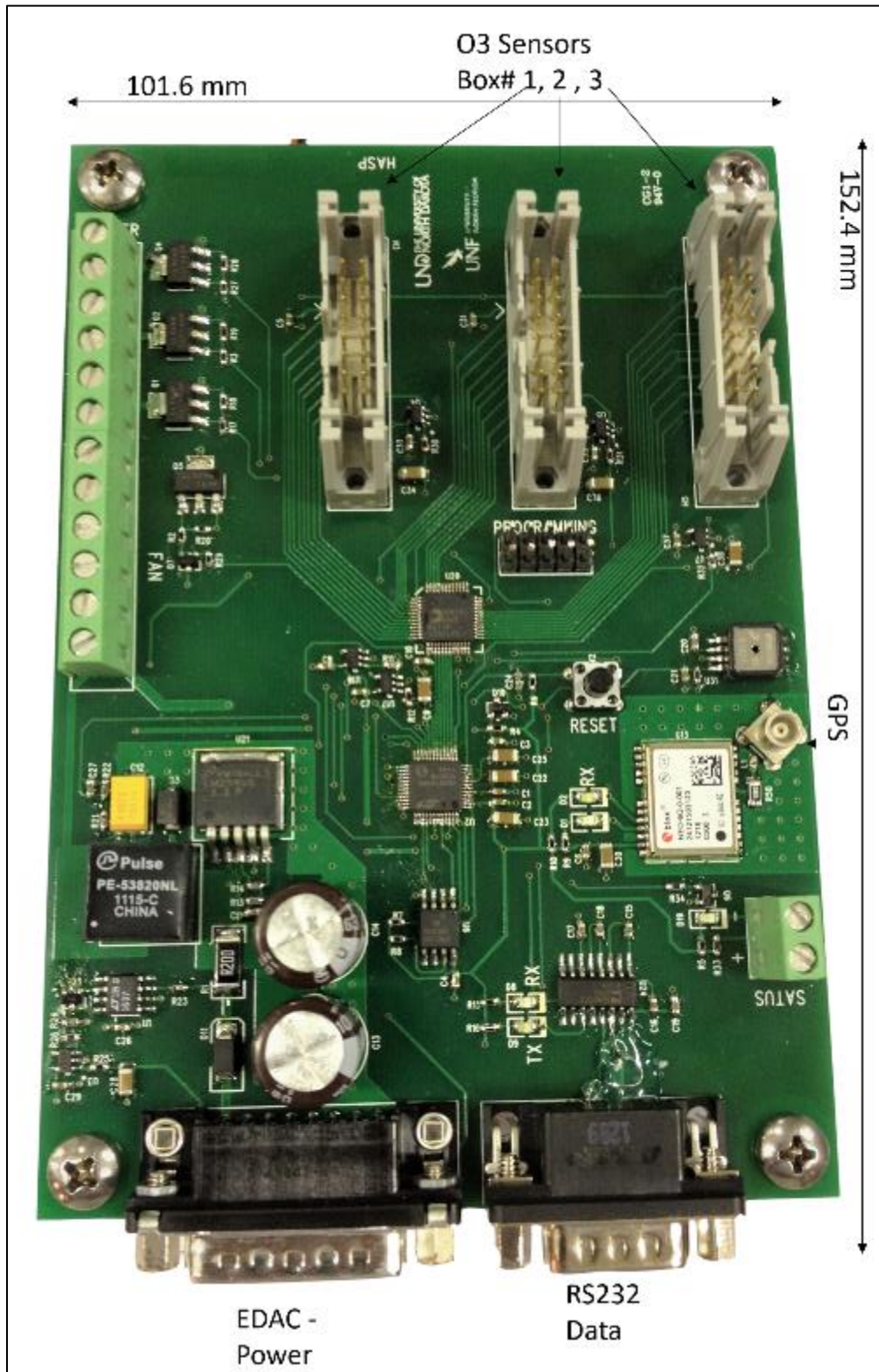


Fig. 6 (i) Picture of microcontroller PCBs

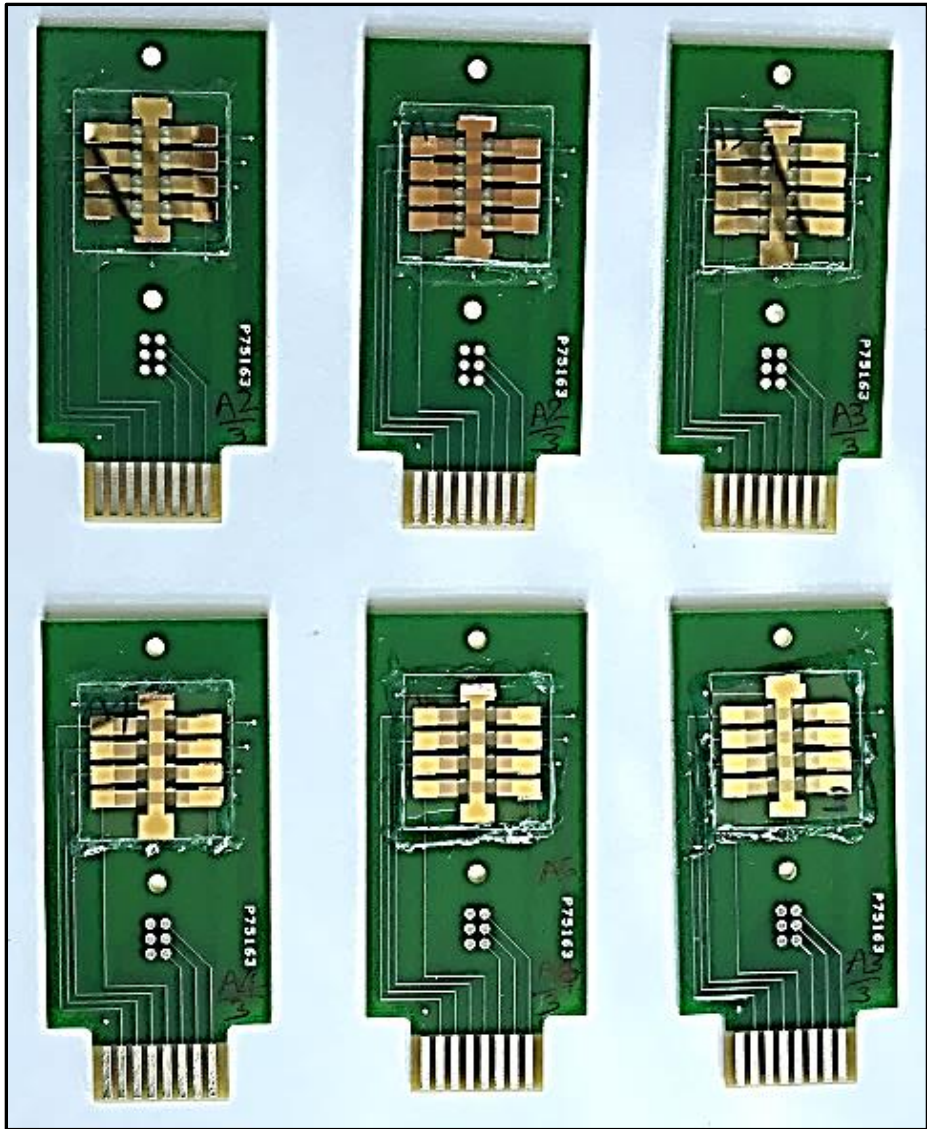


Fig.6 (j) Ozone gas sensor arrays mounted on the PCB

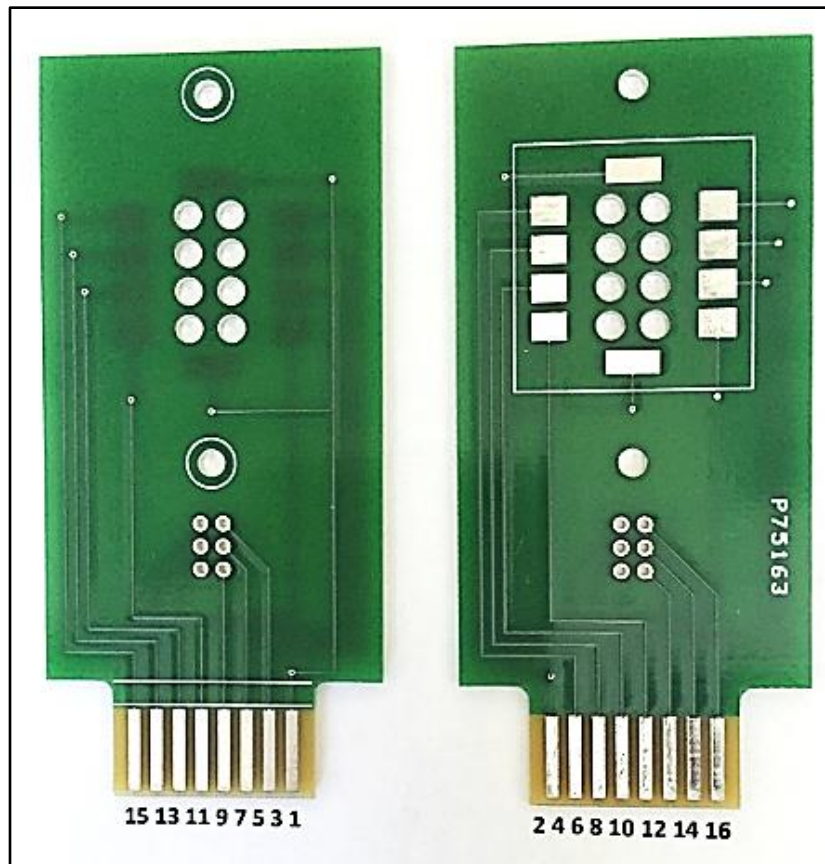


Fig.6 (k) Pin numbers of sensor PCB.

Pin number per connector datasheet							
1	3	5	7	9	11	13	15
Common	Temp Sensor	Temp Sensor	Temp Sensor	Gas Sensor	Gas Sensor	Gas Sensor	Gas Sensor
Open	Gas Sensor	Gas Sensor	Gas Sensor	Gas Sensor	Light Sensor	Light Sensor	Pin not used
2	4	6	8	10	12	14	16
Pin number per connector datasheet							

Fig.6 (l) Pin information for connection of 16 pins female card edge connector with sensor PCB

Information of Components

MINCO Heater

<http://www.minco.com/heater-configurator/model.aspx?PN=HK5573>

Resistance of heater=30 ohms (4.8 Watts)

Acrylic PSA operating voltage =3 to 9 volts

Generate about 100 °C at about 8.00 to 9.00V

FAN

<http://www.digikey.com/product-search/en?lang=en&site=us&Keywords=259-1573-ND>

MC25060V2-000U-A99

Digi-Key Part Number	259-1573-ND
Manufacturer	Sunon Fans
Manufacturer Product Number	MC25060V2-000U-A99
Supplier	Sunon Fans
Description	FAN AXIAL 25X6.9MM 5VDC WIRI
Detailed Description	Fan Tubeaxial 5VDC Square - 25mm L x 25mm H Vapo-Bearing™ 2.2 CFM (0.061m³/min) 2 Wire Leads



Card Edge Connector- Make: 3M

MCS16K-ND

16 pins female to connect Sensor PCB

<http://www.digikey.com/product-search/en?lang=en&site=us&Keywords=MCS16K-ND>



Socket connector, Make: 3M

16 pin female to connect microcontroller PCB

<http://www.digikey.com/product-search/en?lang=en&site=us&Keywords=3452-6600>



Connector, Make: 3M

16 male pin Header – to be mounted on microcontroller PCB

<http://www.digikey.com/product-detail/en/3408-6002/MHS16K-ND/138490>



Low Voltage Temperature Sensors

TMP35/TMP36/TMP37

FEATURES

- Low voltage operation (2.7 V to 5.5 V)
- Calibrated directly in °C
- 10 mV/°C scale factor (20 mV/°C on TMP37)
- ±2°C accuracy over temperature (typ)
- ±0.5°C linearity (typ)
- Stable with large capacitive loads
- Specified –40°C to +125°C, operation to +150°C
- Less than 50 µA quiescent current
- Shutdown current 0.5 µA max
- Low self-heating
- Qualified for automotive applications

APPLICATIONS

- Environmental control systems
- Thermal protection
- Industrial process control
- Fire alarms
- Power system monitors
- CPU thermal management

FUNCTIONAL BLOCK DIAGRAM

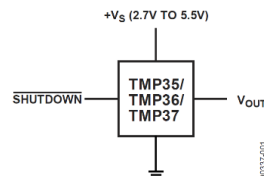


Figure 1.

PIN CONFIGURATIONS

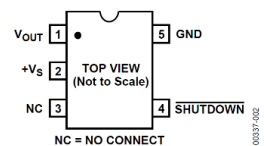


Figure 2. RJ-5 (SOT-23)

